

33598

DYNAMIC ANALYSIS OF TOWER STRUCTURES
A CASE STUDY :PTT KARS TELEVISION TOWER

A Master's Thesis

Presented by

Mustafa TUNCER

to

the Graduate School of Natural and Applied Sciences

of Middle East Technical University

in Partial Fulfillment for the Degree of

MASTER OF SCIENCE

in

CIVIL ENGINEERING

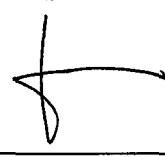
MIDDLE EAST TECHNICAL UNIVERSITY

ANKARA

February, 1993

**T.C. YÜKSEKÖĞRETİM KURULU
DOKÜMANTASYON MERKEZİ**

Approval of the Graduate School of Natural and Applied Sciences.



Prof. Dr. Alpay ANKARA
Director

I certify that this thesis satisfies all the requirements as a thesis for the degree of Master of Science.



Prof. Dr. Doğan ALTINBİLEK
Chairman of the Department

We certify that we have read this thesis and that in our opinion it is fully adequate, in scope and quality, as a thesis for the degree of Master of Science in Civil Engineering.



Prof. Dr. Çetin YILMAZ
Supervisor

Examining Committee in Charge :

Prof. Dr. Nuri AKKAŞ



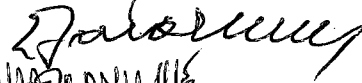
Prof. Dr. Çetin YILMAZ



Doç. Dr. Uğur POLAT



Dr. Erhan KARAESMEN



Yüksek Mühendis Nejat BAYÜLKE



ABSTRACT

DYNAMIC ANALYSIS OF TOWER STRUCTURES A CASE STUDY :PTT KARS TELEVISION TOWER

TUNCER, Mustafa

M.Sc. in C.E.

Supervisor : Prof.Dr. Çetin Yılmaz

February 1993,129 Pages

Structural analysis of PTT Kars Television Tower made both by using computer program Structural Analysis Program SAP90 and by equivalent static calculations using elementary beam theory.

Dynamic properties held by Ambient Vibration Experiment compared with the results of SAP90 computer model. It was observed that approximately the same results were obtained. It shows that, the computer model may generate correct results.

Dynamic and equivalent static calculations are compared. The results are completely different. Previous wind calculations made by the vendor are examined and the load results are compared.

It may be predicted that, the reason of the collapse is the underestimation of the dynamic loads and for special kind of structures like towers, dynamic loads are important and dynamic analysis should be held.

Key words : Tower Shaped Structures, Multi Element Structures, Vibrational Characteristics, Dynamic Properties, Structural Analysis, Equivalent Static Calculations

Science Code : 620.01.01

ÖZ

KULE TİPİ YAPILARIN DİNAMİK ANALİZİ

PTT KARS TELEVİZYON VERİCİ KULESİ

TUNCER, Mustafa

Yüksek Lisans Tezi, İnşaat Mühendisliği Anabilim Dalı

Tez Yöneticisi : Prof.Dr. Çetin Yılmaz

Şubat 1993,129 Sayfa

PTT Kars Televizyon Verici Kulesi analizi, SAP90 Yapı Analiz Programı ile bilgisayarda dinamik olarak ve çeşitli eşdeğer statik yükleme standartları kullanılarak statik olarak ele alındı.

SAP90 yapı analiz programı ile serbest titreşim deneyi sonuçlarından elde edilen dinamik özellikler karşılaştırıldı. Sonuçların birbirlerine yakınlığı gözlemlendi.

Dinamik ve statik analizler karşılaştırıldı. Sonuçların tamamen farklı

olduđu gözlendi. Yapı ile ilgili daha önceden yapılmıř statik rüzgar hesapları incelendi ve karşılařtırmalar yapıldı.

Binanın zarar görme sebebinin, dinamik yüklerin ihmal edilmesi olabileceđi düşünöldü. Kule tipi yapılar gibi özel binalarda, dinamik analiz yapılması gerekliliđi gözlendi.

Anahtar sözcükler : Kule Tipi Yapılar, Deđişik Yapı Malzemeleri İle İmal Edilen Yapılar, Titreřim ve Dinamik Özellikler, Yapı Analizi, Eřdeđer Statik Yüklemeler

Bilim Kodu : 620.01.01

ACKNOWLEDGEMENTS

This study was suggested by Prof.Dr.Çetin YILMAZ and the work has been carried out under his supervision in the Department of Civil Engineering at the Middle East Technical University. I gratefully acknowledge his advice, patient supervision, and tolerance.

Dr. Erhan KARAESMEN is also gratefully acknowledged for his detailed and helpful comments.

I owe thanks to by bosses İsmail SALICI and Hasan ÖZDEMİR for their tolerance at Prokon and my family, my office friends Gülay KIR, Ömer ÇETİNKAYA and Ümit KAZAK for their helps those encouraged me during all of the study.

This work is dedicated to my father M.İsfendiyar TUNCER, who supported me for being a civil engineer and dedicated his life to me.

TABLE OF CONTENTS

| | Page |
|--|------|
| ABSTRACT | iii |
| ÖZ | v |
| ACKNOWLEDGEMENT | vii |
| LIST OF TABLES | xi |
| LIST OF FIGURES | xiii |
| NOMENCLATURE | xvi |
| | |
| CHAPTER I : INTRODUCTION | 1 |
| 1.1. General | 1 |
| 1.2. Problem | 2 |
| 1.3. Scope | 3 |
| | |
| CHAPTER II : LITERATURE SURVEY | 4 |
| | |
| CHAPTER III : DESCRIPTION OF THE STRUCTURE | 6 |
| 3.1. General | 6 |

| | Page |
|---|------|
| CHAPTER IV : FINITE ELEMENT MODEL OF THE STRUCTURE . . . | 13 |
| 4.1. General | 13 |
| 4.2. Material and Element Properties | 32 |
| 4.3. Previous Investigations | 37 |
| 4.4. Evaluation of Results | 38 |
| 4.5. Time Domain Analysis | 39 |
| 4.6. Response Spectrum Analysis | 51 |
| 4.7. Discussion | 53 |
| | |
| CHAPTER V : EQUIVALENT STATIC CALCULATIONS | 57 |
| 5.1. General | 57 |
| 5.2. Design of Connections | 59 |
| 5.3. Equivalent Lateral Force Procedure | 60 |
| 5.3.1. ATC 3-06 for Earthquake Resistant Structures | 61 |
| 5.3.2. Turkish Code for Earthquake Resistant Structures | 65 |
| 5.4. Cantilever Method | 67 |
| 5.5. Strength Difference Method | 69 |
| 5.6. Japanese Practice | 70 |

| | Page |
|--|------|
| CHAPTER VI : DISCUSSION OF THE RESULTS AND CONCLUSION . | 73 |
| 6.1. The Wind Loading Calculations by the Vendor | 73 |
| 6.2. Dynamic Analysis by Computer | 74 |
| 6.3. Equivalent Static Calculations | 75 |
| 6.4. Conclusion | 76 |
| REFERENCES | 81 |
| APPENDICES | |
| APPENDIX A. DYNAMIC ANALYSIS BY STRUCTURAL ANALYSIS | |
| PROGRAM SAP90 | 84 |
| A.1. Mode Superposition Method | 84 |
| A.2. Calculations of Frequencies and Mode Shapes | 88 |
| A.3. The Determinant Search Solution | 89 |
| A.4. The Supspace Iteration Solution | 90 |
| A.5. Dynamic Analysis | 92 |
| A.6. Response History Analysis by Mode Superposition | 93 |
| A.7. Response History Analysis by Direct Integration | 94 |
| APPENDIX B. COMPUTER INPUT FOR SAP90 | 98 |

LIST OF TABLES

| | Page |
|--|------|
| Table 3.1. Properties of Steel Cylinder | 8 |
| Table 3.2. Properties of Concrete Cylinder | 9 |
| Table 4.1. Numerical and Experimental Natural Frequencies and Periods . | 39 |
| Table 4.2. Maxima for Different Damping Values | 45 |
| Table 4.3. Spectral Adjustment Factors for Damping | 52 |
| Table 4.4. Maxima Obtained from the Response Spectrum Analysis | 53 |
| Table 4.5. Maximum Moment Occuring at the Bottom of the GRP Antenna | 54 |
| Table 5.1. Loads Along the Tower and Moments with respect to Elevations +0.00m, +14.00m, +30.00m, +60.90m, and +82.10m | 58 |
| Table 5.2. Coefficient Av and Seismicity Index | 59 |
| Table 5.3. Minimum Load that Connections Should Resist | 60 |
| Table 5.4. Lateral Load Distribution Along the Tower According to ATC 3-06 | 64 |

| | Page |
|---|------|
| Table 5.5. Lateral Load Distribution Along the Tower According to Turkish Code | 68 |
| Table 5.6. Shear Capacity of Different Sections Along the Tower | 70 |
| Table 5.7. Revised Lateral Loads Along the Tower with respect to Height | 72 |
| Table 6.1. Comparison of Test and Computer Results | 74 |
| Table 6.2. Comparison of Equivalent Static Calculations | 76 |
| Table 6.3. Maximum Moment Occuring at the Bottom of the GRP Antenna | 77 |
| Table A.1. Step-by-Step Direct Integration Algorithm | 96 |

LIST OF FIGURES

| | Page |
|--|------|
| Figure 3.1. General Outline of the Tower | 10 |
| Figure 3.2. Summary of the Geometry of the Tower | 11 |
| Figure 3.3. Geometry of GRP Antenna | 12 |
| Figure 4.1. Finite Element Layout at +3.00m Elevation | 14 |
| Figure 4.2. Model of the Structure with Shear Walls | 16 |
| Figure 4.3. Model of the Structure : General View | 17 |
| Figure 4.4. General View of the Model of the Building Part | 18 |
| Figure 4.5. Model of the building part Showing Foundation Fix Restraints . | 19 |
| Figure 4.6. Model of the Building Part Showing Node Point Numbering ... | 20 |
| Figure 4.7. Model of the Building Part Showing Shear Walls | 21 |
| Figure 4.8. Model of the Structure between +10.00m ~ +20.00m Elevations Showing Node and Element Numbering | 22 |
| Figure 4.9. Model of the Structure between +10.00m ~ +20.00m Elevations Showing Node and Element Section Property Numbering | 23 |
| Figure 4.10. Model of the Structure between +20.00m ~ +40.00m Elevations Showing Node and Element Numbering | 24 |

| | |
|---|----|
| Figure 4.11. Model of the Structure between +20.00m ~ +40.00m Elevations Showing Node and Element Section Property Numbering | 25 |
| Figure 4.12. Model of the Structure between +40.00m ~ +60.00m Elevations Showing Node and Element Numbering | 26 |
| Figure 4.13. Model of the Structure between +40.00m ~ +60.00m Elevations Showing Node and Element Section Property Numbering | 27 |
| Figure 4.14. Model of the Structure between +60.00m ~ +80.00m Elevations Showing Node and Element Numbering | 28 |
| Figure 4.15. Model of the Structure between +60.00m ~ +80.00m Elevations Showing Node and Element Section Property Numbering | 29 |
| Figure 4.16. Model of the Structure between +80.00m ~ +96.00m Elevations Showing Node and Element Numbering | 30 |
| Figure 4.17. Model of the Structure between +80.00m ~ +96.00m Elevations Showing Node and Element Section Property Numbering | 31 |
| Figure 4.18. First Vibration Mode Shapes | 40 |
| Figure 4.19. Second Vibration Mode Shapes | 41 |
| Figure 4.20. Third Vibration Mode Shapes | 42 |
| Figure 4.21. Fourth Vibration Mode Shapes | 43 |
| Figure 4.22. Time History Function of Computer Model versus Time | 46 |
| Figure 4.23. Base acceleration at XT Direction versus Time | 47 |

| | Page |
|---|------|
| Figure 4.24. Acceleration of Node 590 at XT Direction versus Time | 48 |
| Figure 4.25. Acceleration of Node 596 at XT Direction versus Time | 49 |
| Figure 4.26. Displacement of Node 596 at XT Direction versus Time | 50 |
| Figure 4.27. Near Field Response Spectrum (5% damping) | 55 |
| Figure 4.28. Far Field Response Spectrum (5% damping) | 56 |



NOMENCLATURE

| | |
|---------------|---|
| A_v | seismic coefficient representing the Effective Peak Velocity-Related Acceleration |
| c | damping coefficients |
| C | seismic design coefficient |
| C_0 | seismic zone coefficient |
| C_d | the deflection amplification factor |
| C_{vn} | lateral load coefficient for nth level |
| \tilde{C}_d | modified deflection amplification factor |
| D | width of the building at the foundation level |
| F_b | seismic base shear |
| F_n | lateral seismic force at nth level |
| F_t | lateral load applied on the top level of the structure |
| h_n | the height in feet above the base to the highest level of the building |
| H | height of the building |
| I | structural importance coefficient |
| k | spring constants |
| k_{ij} | stiffness influence coefficients |
| K | building type coefficient |
| K_n | generalized stiffness of nth normal mode |

| | |
|-------------|---|
| L | the overall length in feet of the building at the base in the direction under consideration |
| m | mass |
| M_n | generalized mass of nth normal mode |
| $p(t)$ | forcing function |
| r_n | ratio of shear capacity to design shear for nth level |
| R | the seismic response modification factor |
| \tilde{R} | modified seismic response modification factor |
| S | coefficient for the soil profile characteristics, or structural dynamic |
| T | the fundamental period of the building |
| T_a | the approximate fundamental period for the building |
| u | displacement |
| \dot{u} | velocity |
| \ddot{u} | acceleration |
| v_o | iteration starting vector |
| V | vector |
| w | undamped natural circular frequency |
| W | total weight of the building |
| ϕ_n | nth mode shape |
| \cap | principal coordinates |

Ω eigenvalue diagonal matrix
 Φ orthonormalized eigenvectors matrix



CHAPTER I

INTRODUCTION

1.1. General

After the collapse of the top GRP(Glass Reinforced Plastic) element of PTT Kars Broadcasting Tower, following the Spitak (Armenian) Earthquake of December 7th, 1988, owner of the antenna PTT began to investigate the case. The interesting side of the collapse was that no other building had any damage during the earthquake but only the top portion of the antenna structure. The collapse was at the connection of the GRP antenna to the tower structure.

It was thought that some special dynamic characteristics of the tower may arouse the collapse. The glass fiber reinforced cylinders, supporting the 2nd channel TV antennas of KARS TV station, was at the top of previously built 85 meter high tower. The tower has three main parts:

1. A cylindrical shaped, reinforced concrete accommodation building

2. A cylindrical shaped, reinforced concrete variable section tower placed at the core of the accommodation building
3. A cylindrical shaped steel tower at the top of the reinforced concrete tower.

A detailed soil investigation, geological and technical specifications prepared by another team at METU and the ambient vibration of Kars Television Tower have been measured on November 7-8, 1990.

1.2. Problem

The GRP antenna was carefully investigated by Alan Dick & Company Limited of England for wind load affects and it was stated that lateral seismic affects are not governing for the antenna. Lateral load analysis of the antenna was held by taking the GRP section alone and load affects coming from the dynamic characteristics of the tower structure may be underestimated.

Yılmaz, Erdik and Akkaş [18] stated that "Analysis of the GRP section has been held as a separate structure in the calculations by the vendor and no interaction with the tower structure is considered. This error in the calculation is underestimate the structural stresses during dynamic loadings."

1.3. Scope

The dynamic characteristics of the Kars TV Antenna Structure have been measured by another team at METU and the ambient vibration of the tower have been measured.

In this paper, the finite element model of the structure is studied and dynamic characteristics are held. The tower was defined like a cantilever bar, that is fixed at the base, so the computer model was not a structurally well detailed model but the mass along the tower are modelled in detail. It is tried to be perfect on mass of the structure. The results of tests and mathematical model are compared.

After comparison of the frequency results of test and mathematical model, load effects at some critical points of the tower are investigated. In this study, the dynamic properties of the tower are investigated by the use of a computer model and results are compared with equivalent static load design algorithms.

CHAPTER II

LITERATURE SURVEY

For the analysis of parabolic cooling towers Arya and Thakkar[13], indicated that the exact nature of the equivalent lateral loads along the height of hyperbolic cooling towers is not known and can only be predicted by dynamic analysis.

Morrone[14] in his investigations on a self supporting stack had shown the practical accuracy of using the lumped parameter method to determine the fundamental frequency.

Radhakrishnan[16] studied the response to transient excitation with the effects of additional constrained masses and suggested that the inherent structural damping in the structure is the controlling parameter on the maximum stresses and deformations when subjected to dynamic loads. In his studies, it is concluded that

a.The use of elementary beam theory predicts the principal natural bending modes and frequencies quite closely for the case of triangulated frame tower structure.

b.The damping characteristics demonstrate an important difference in the damping factors associated with bending and torsional modes.

c.The oscillation decay method indicated a variation of damping factor with oscillation amplitude number.

Newton[17], while analyzing a tower model, has found that beam theory predicts results quite close with the experimental values of frequencies and mode shapes, but does not give any indication of the increasing complexity of the motion as the forcing function increases. He investigated the variation of damping with oscillation amplitude using the energy dissipation method. He concluded that theoretical models for the damping mechanisms, typical of the tower frame work should be of the form of equation but taking into account the fact that the damping index itself increases overall stress amplitude.

CHAPTER III

DESCRIPTION OF THE STRUCTURE

3.1. General

PTT Kars TV Antenna is designed to serve as a TV broadcasting antenna, shelter for equipment and accommodation for workers. The Kars TV tower is a multi material building : a concrete building at the base, a reinforced concrete circular wind shield, and a steel circular cylinder with the GRP cylinder mounted on the top.

Tower, has two main parts. First is a 5 story cylindrical shelter and accommodation building between +0.00 and +14.10 elevations and second is a cylindrical tower structure which is placed inside of the first structure eccentrically.

The shelter and accommodation structure is $R=14\text{m}$ cylindrically shaped, 5 story reinforced concrete structure. Floor elevations are +0.000m, +3.000m,

+5.400m, +8.600m, +11.300m and +14.100m. +14.100m elevation is the terrace floor and staying broadcasting antenna equipments. Other floors are used for accomodation of technicians and broadcasting equipments.

The tower structure has 6 different structural geometry with three different type of structural material, placed inside of the shelter structure eccentrically : reinforced concrete, steel, and GRP materials placed on each other. The properties of the steel cylinder which is between levels 67.20m and 82.10m are tabulated in Table 2.1 and the cross section and some geometrical properties of reinforced concrete section are tabulated in Table 3.2.

a. Between +0.000m and +14.100m elevations, a 35cm thick reinforced concrete cylindrical shear wall, which is also serving as ladder tower for shelter and accomodation building.

b. Between +14.100m and +26.000m elevations, a 25cm thick reinforced concrete cylindrical shear wall with outer radius of 4.50m.

c. Between +26.000m and +30.000m elevations, a 150cm thick reinforced concrete cylindrical passing zone with outer radius of 4.50m.

Table 3.1 Properties of Steel Cylinder

| Level | Length (m) | r_i (m) | t_i (mm) | F (m ²) | I (m ⁴) x10 ⁻⁶ |
|---------------|---------------|--------------|---------------|------------------------|---|
| 76.20 ~ 82.10 | 5.90 | 0.60 | 8 | 0.03036 | 5538.2 |
| 67.20 ~ 76.20 | 9.00 | 0.60 | 10 | 0.03801 | 6957.4 |
| 64.20 ~ 67.20 | 3.00 | 0.60 | 14 | 0.05339 | 9837.9 |
| 60.90 ~ 64.20 | 3.30 | 0.60 | 16 | 0.06112 | 11299.4 |

d. Between +30.000m and +60.900m elevations variable section cylindrical shear wall: at +30.000m elevation with outer radius of 2.40m and 45cm wall thickness; at 60.900m elevation with outer radius of 2.40m and 30cm wall thickness.

e. Between +60.900m and +82.100m elevation, a 18mm thick cylindrical steel plate wall with inner radius of 1.20m.

f. Over +82.100m GRP TV antenna structure.

Table 3.2 Properties of Concrete Cylinder

| Level | Length h (m) | r_o (m) | t_{lower} (m) | t_{top} (m) | F_{ay} (m ²) | I_{ay} (m ⁴) |
|---------------|--------------------|--------------|--------------------|------------------|-------------------------------|-------------------------------|
| 54.00 ~ 60.90 | 6.90 | 1.15 | 0.30 | 0.30 | 1.884955 | 0.963683 |
| 48.00 ~ 54.00 | 6.00 | 1.15 | 0.30 | 0.30 | 1.884955 | 0.963683 |
| 42.00 ~ 48.00 | 6.00 | 1.15 | 0.30 | 0.30 | 2.016509 | 1.009830 |
| 36.00 ~ 42.00 | 6.00 | 1.15 | 0.30 | 0.30 | 2.267837 | 1.090333 |
| 30.00 ~ 36.00 | 6.00 | 1.15 | 0.30 | 0.30 | 2.503456 | 1.156675 |
| 26.50 ~ 30.00 | 3.50 | 2.25 | 0.30 | 0.30 | 10.178760 | 17.520190 |
| 21.50 ~ 26.50 | 5.00 | 2.25 | 0.30 | 0.30 | 3.337942 | 7.562524 |
| 19.15 ~ 21.50 | 2.35 | 2.25 | 0.30 | 0.30 | 3.337942 | 7.562524 |
| 16.80 ~ 19.15 | 2.35 | 2.25 | 0.30 | 0.30 | 3.337942 | 7.562524 |

On the tower, there are antenna platforms at +23.000m, +30.000m, +60.900m, and +82.100m elevations. Platforms at +23.000m and +30.000m are reinforced concrete and others are structural steel.

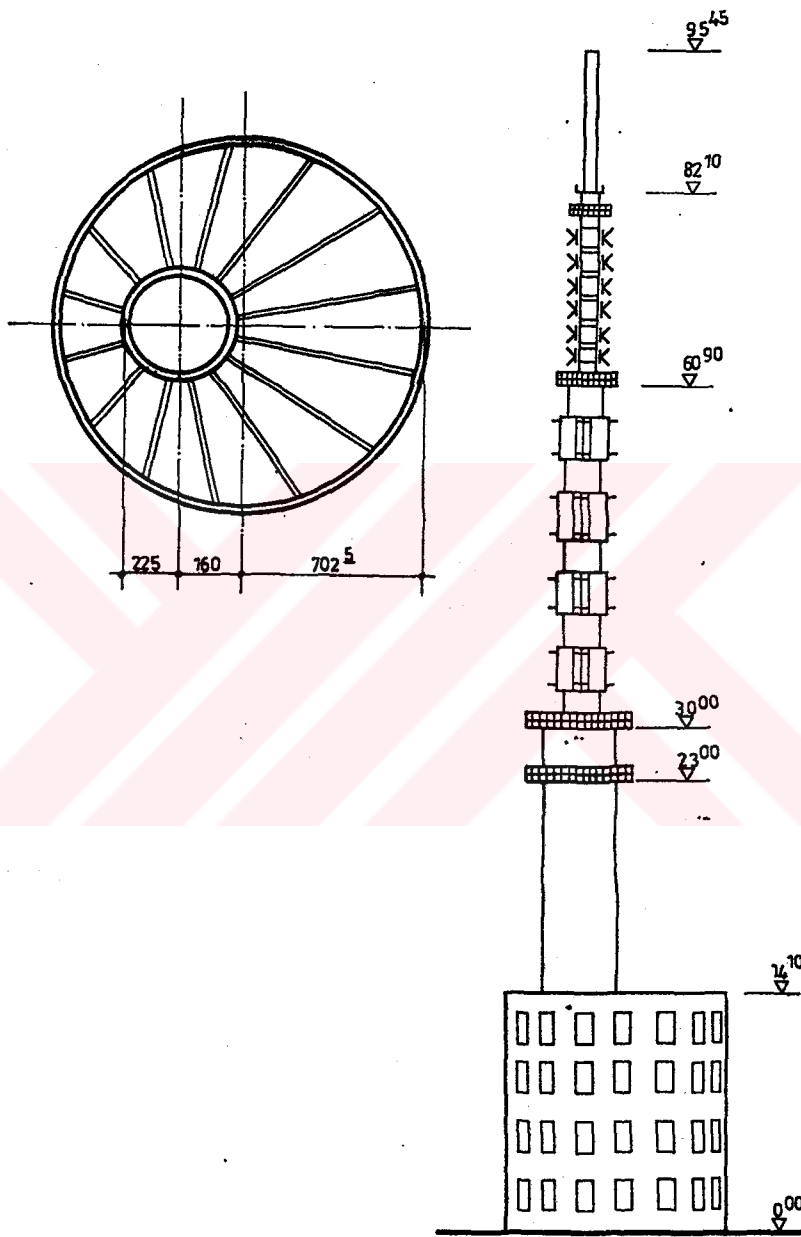


Figure 3.1 General Outline of the Tower

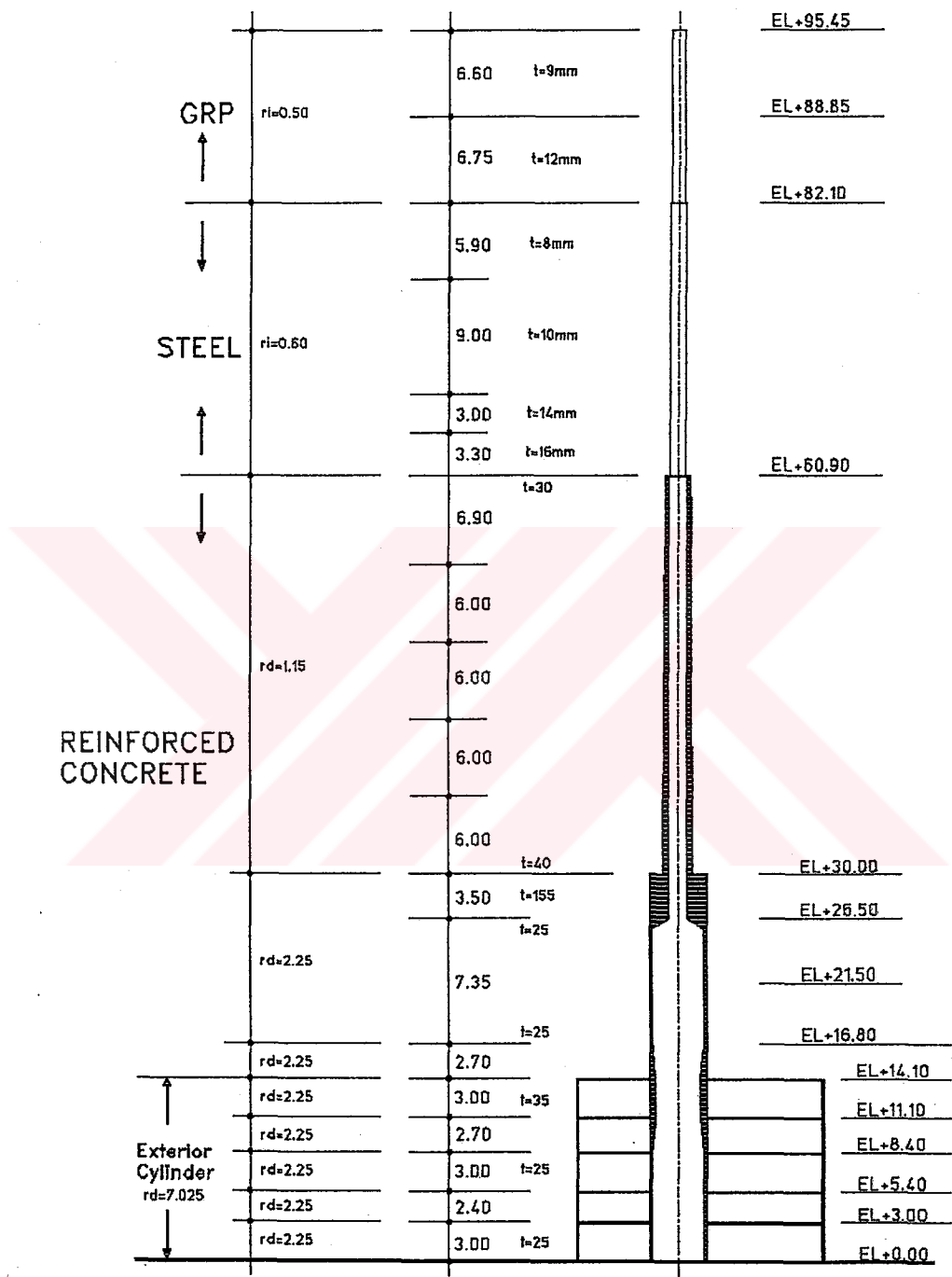


Figure 3.2 Summary of the Geometry of the Tower

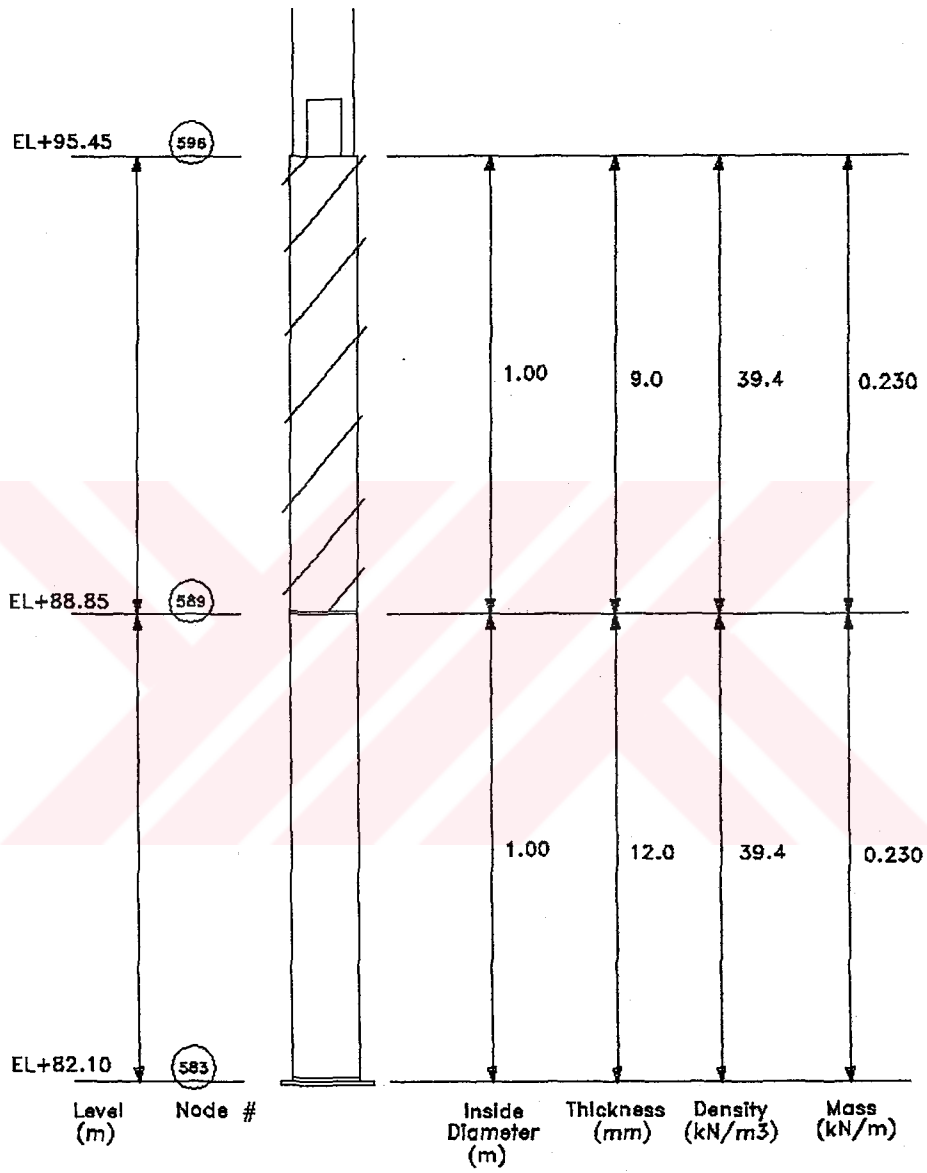


Figure 3.3 Geometry of GRP Part

CHAPTER IV

FINITE ELEMENT MODEL OF THE STRUCTURE

4.1. General

Finite element model of the structure is established by using SAP90 Structural Analysis Program Version 5.10 that have the capability of carrying out static and dynamic earthquake analysis of all kinds for linear structures.

Computer model of the structure is begin at the foundation level (+0.000). At +0.000m elevation, 15 nodal points are modelled for foundation. All nodal point boundary conditions at foundation level is assumed as fixed. The tower structure is modelled as a simple bar, and the foundation of the tower is presented by one node only. This modelling technique is established to minimize the run time for the dynamic analysis.

The building section of the structure has a star shaped beam orientation

inside of the cylindrical shaped outer beams. All dimensions and geometry is modelled using Foundation Formwork Plan and Sections Drawing that is provided by PTT.

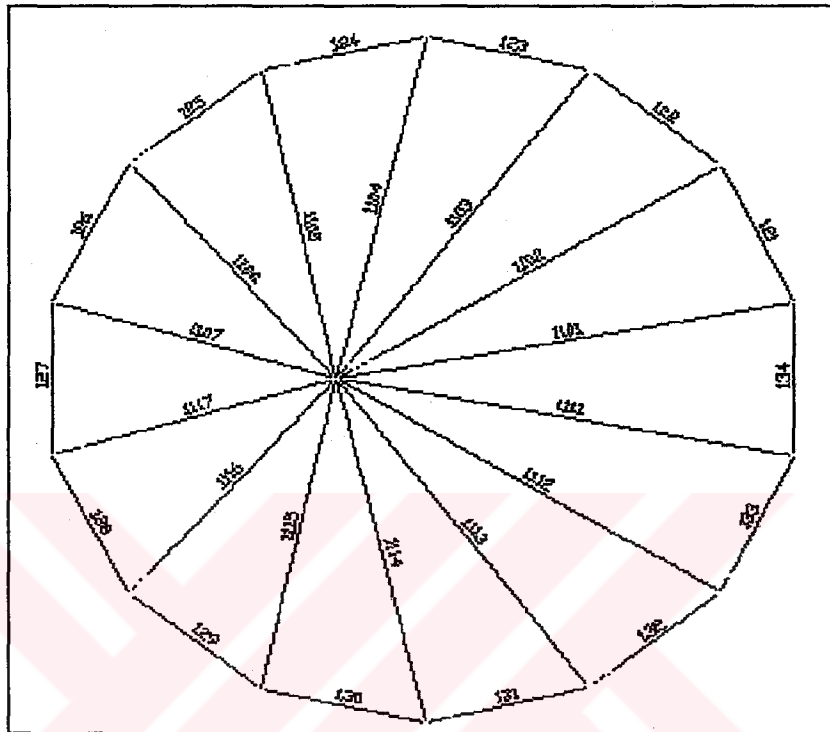


Figure 4.1 Finite Element Layout at +3.00m Elevation

At the model of bottom sections, up to +14.10m elevation, the inner beams are modelled longer than their real lengths. Length of the beams are corrected by defining rigid zones at the inner ends. For each beam that is modelled longer than its real length, rigid zones are defined for the half radius of the tower section.

Outer shear walls of the building section is defined by using shell elements. As the stress values on the shear walls are not of interest to its study, only one shell element is used for every span.

Around the shell elements, 20cmx20cm dummy beams and columns are defined. These dummy frame elements are used to examine the load distribution within the structure. Floors of the building section of the structure is modelled by using constraints at nodal points at floor levels. The lateral displacements of every nodal point at a floor level are constrained.

For all sections of the building the real section properties are defined. Building dead loads are taken into consideration by assigning gravitational loads to the sections. Assumed equipment dead loads are included in the self weights of the building sections.

No special modelling technique is used neither for the model of transition zone from reinforced concrete to steel nor from steel to GRP. For the modelling of antenna weights at +30.000m and +60.900m elevations, additional masses are defined at platform levels. The details of computer model are presented in Figures 4.1 to 4.17.

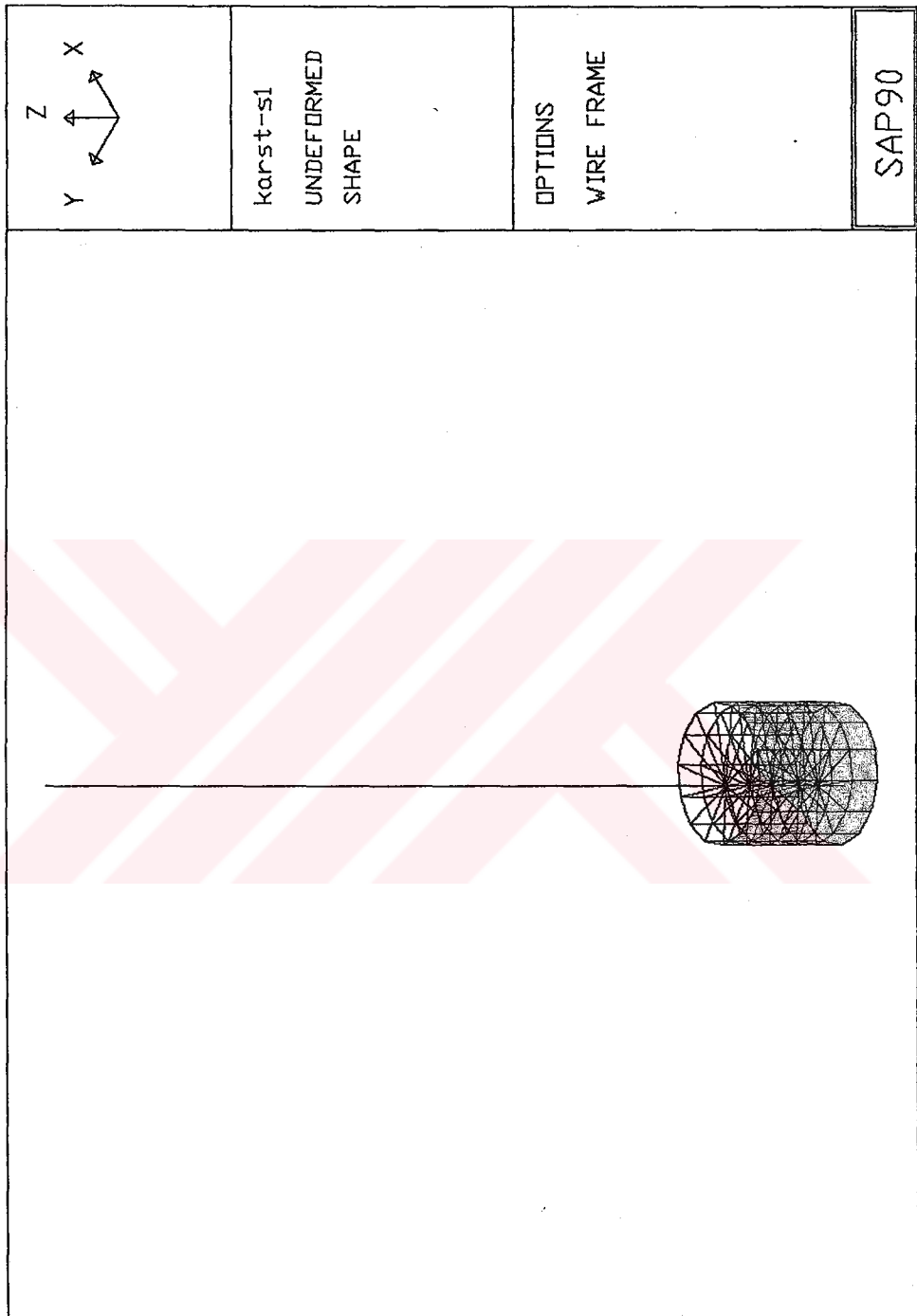


Figure 4.2 Model of the Structure with Shear Walls

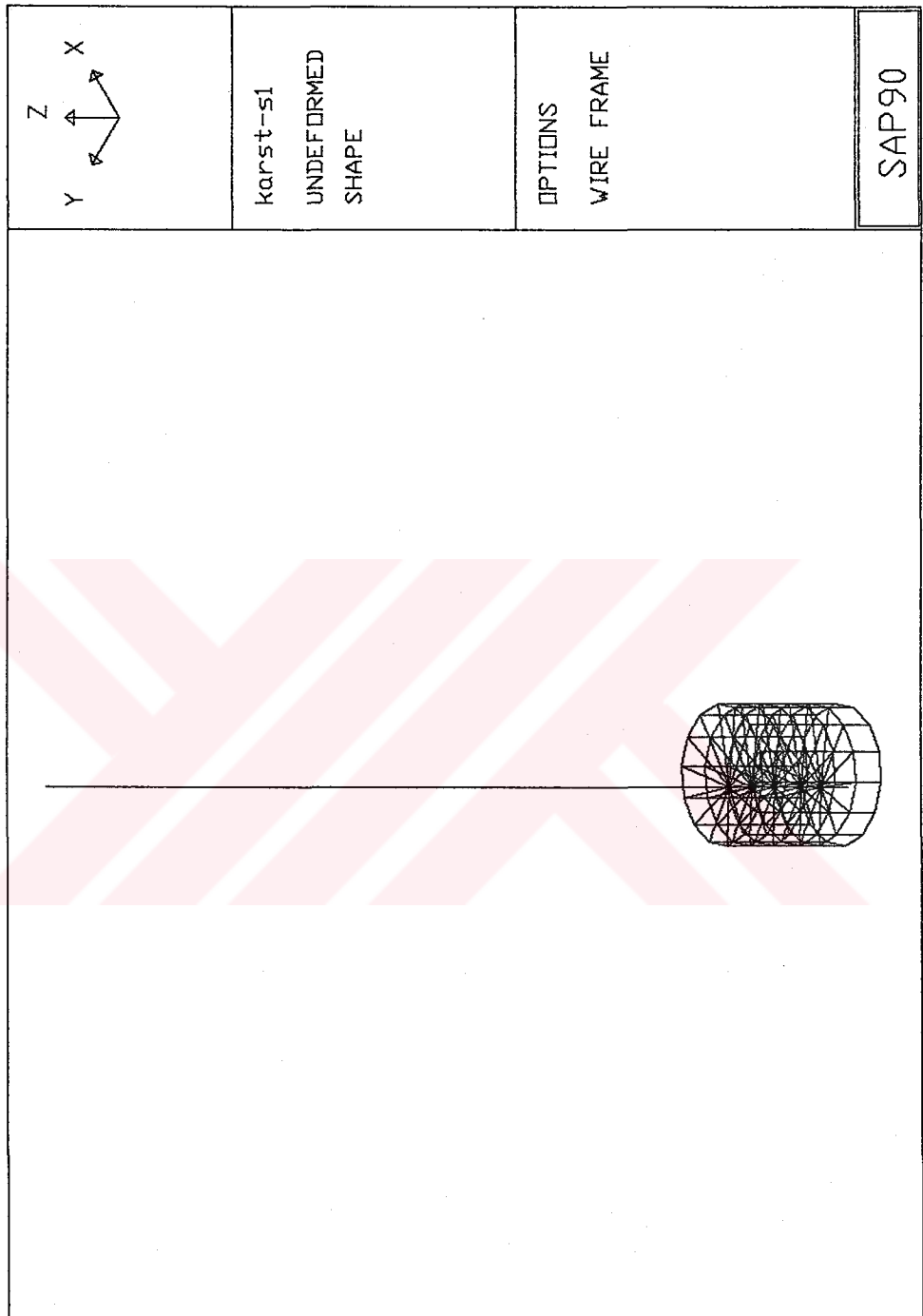


Figure 4.3 Model of the Structure : General View

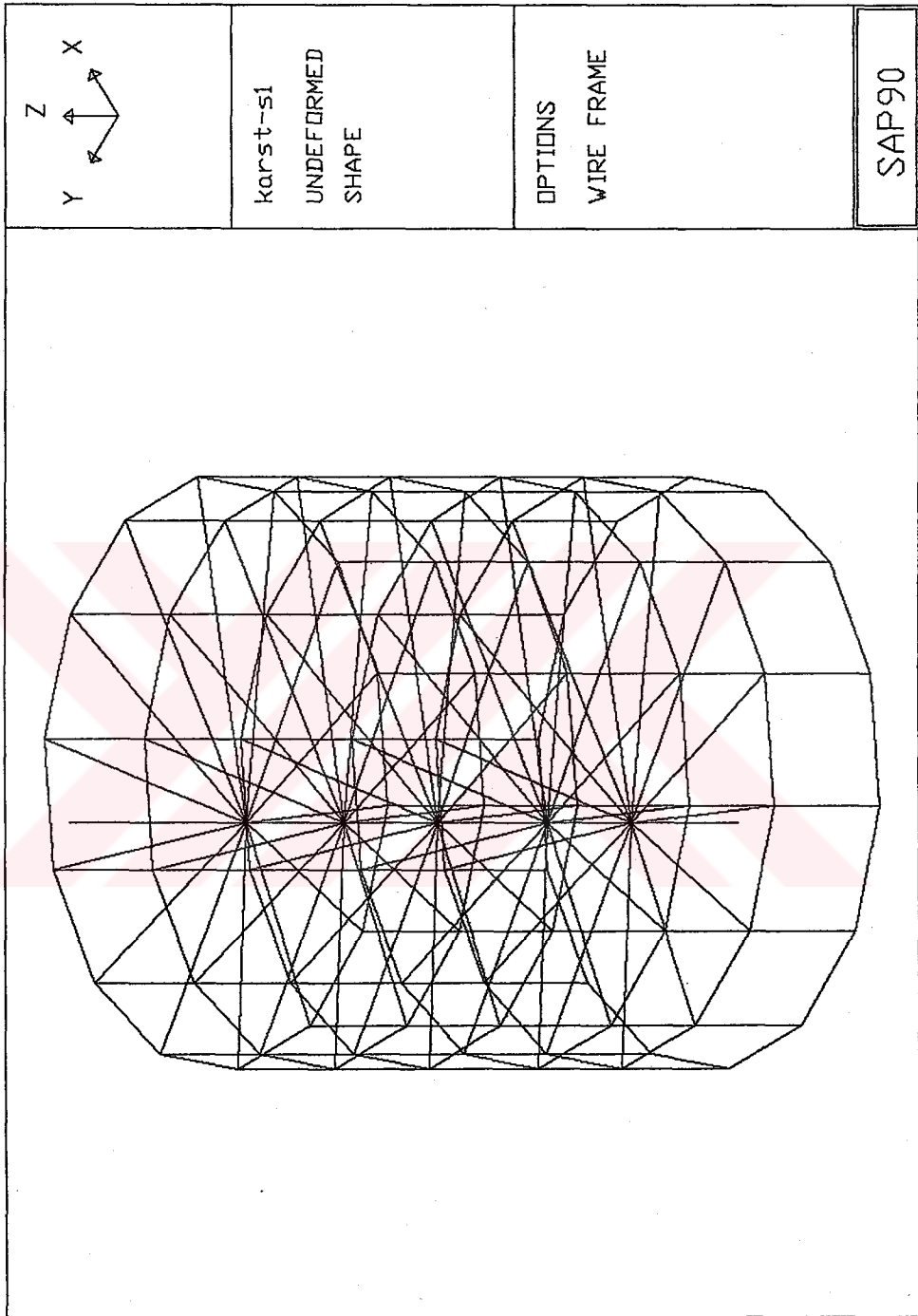


Figure 4.4 General View of the Model of the Building Part

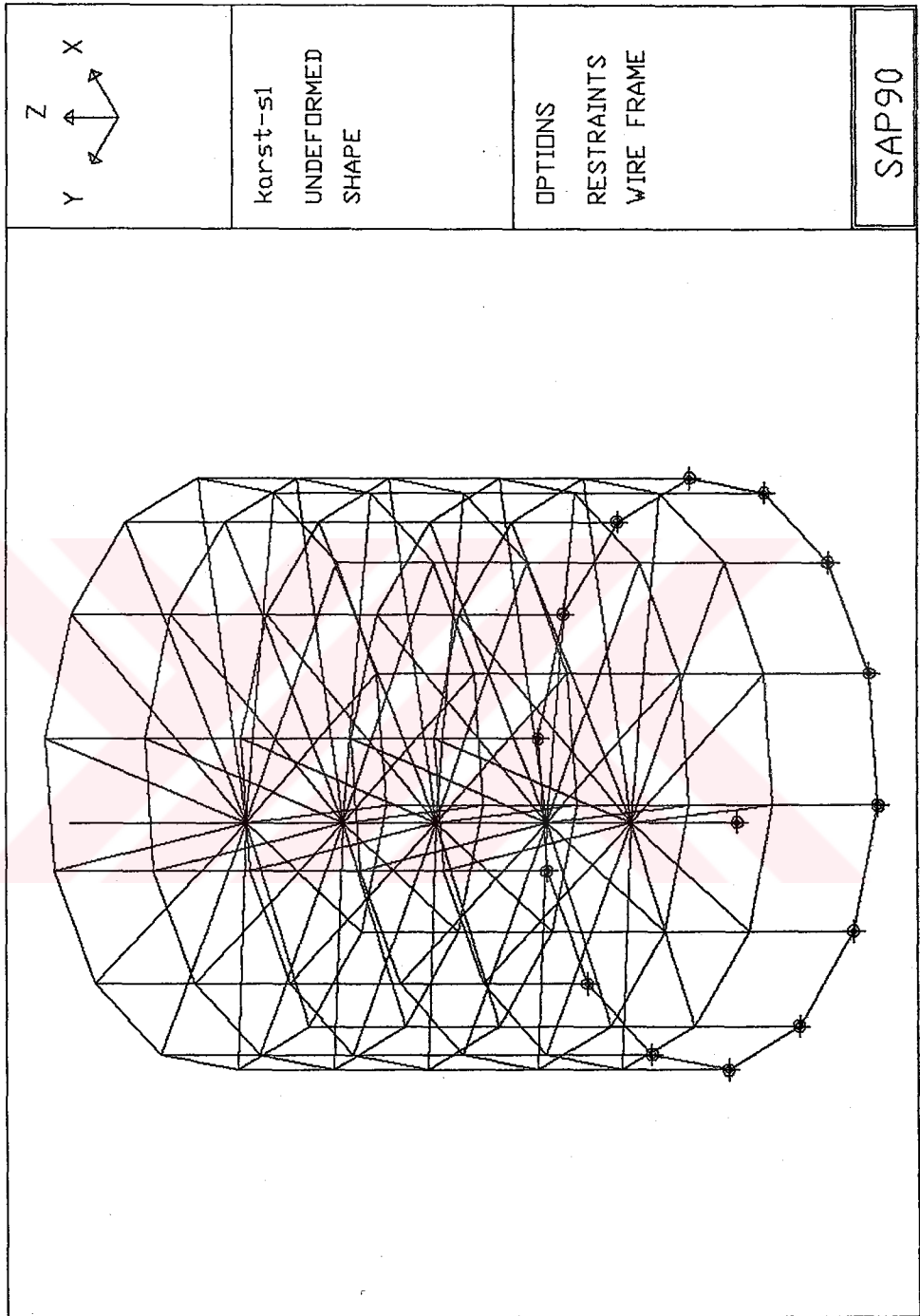


Figure 4.5 Model of the Building Part Showing Foundation Fix Restraints

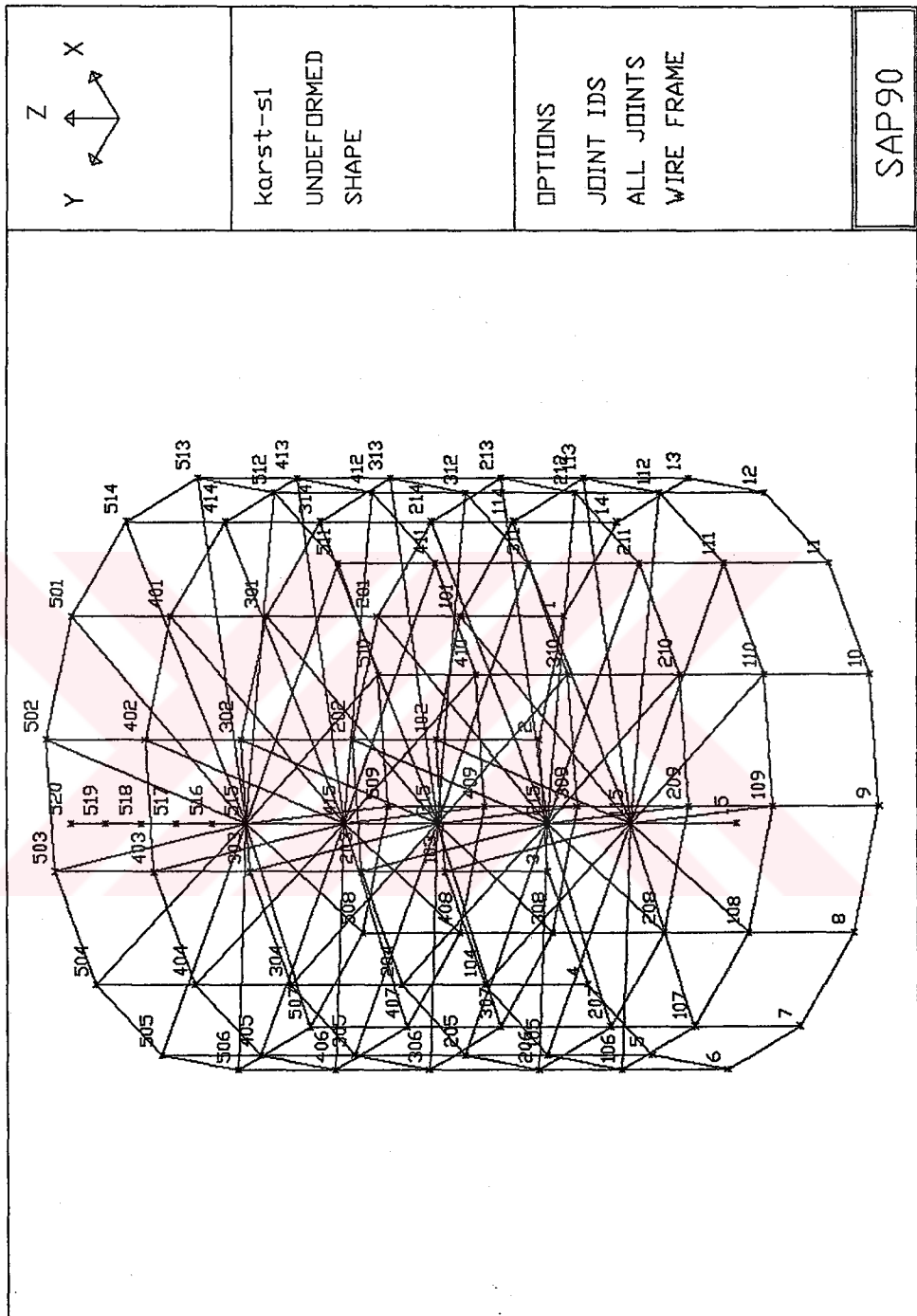


Figure 4.6 Model of the Building Part Showing Nodal Point Numbering

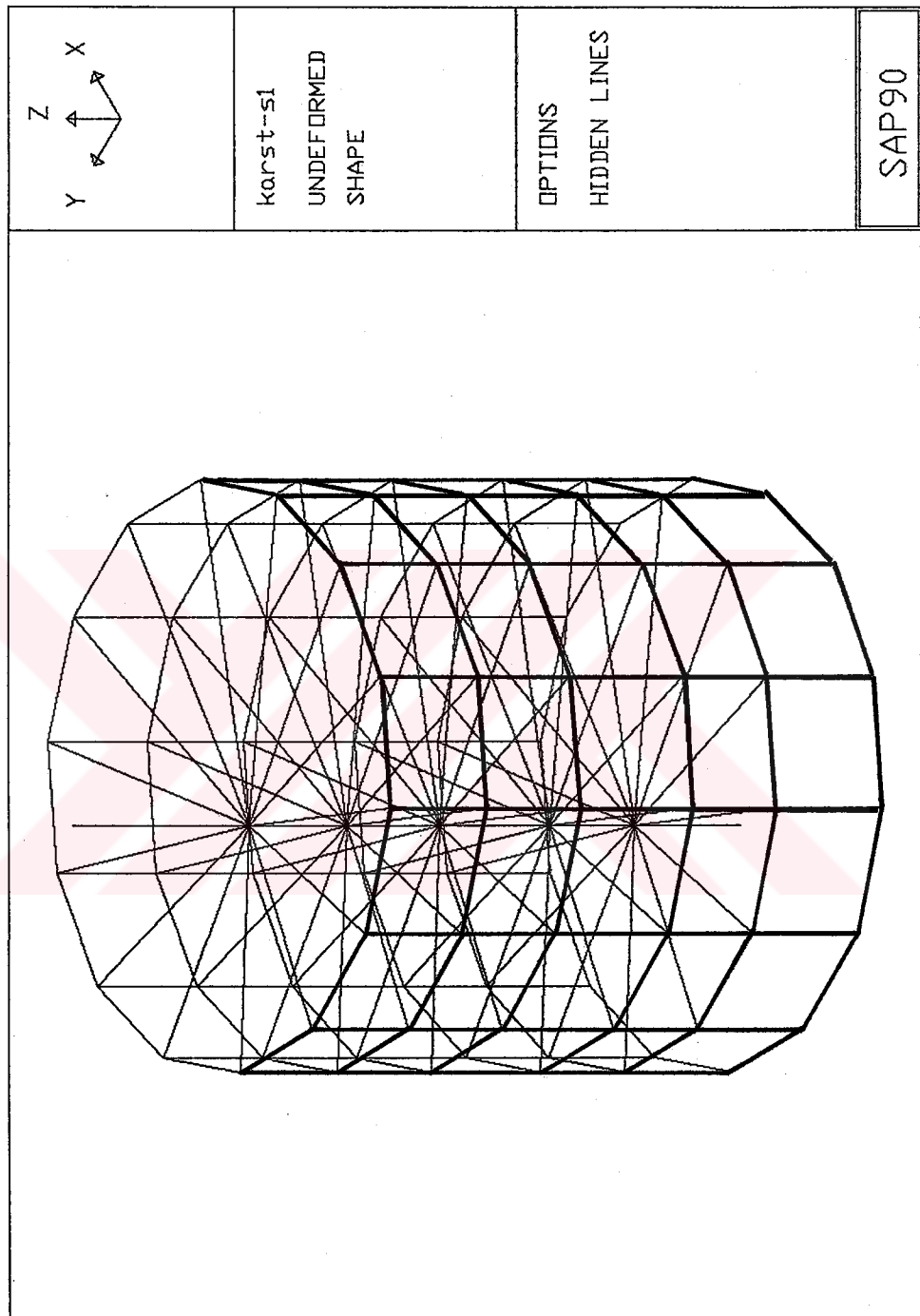


Figure 4.7 Model of the Building Part Showing Shear Walls

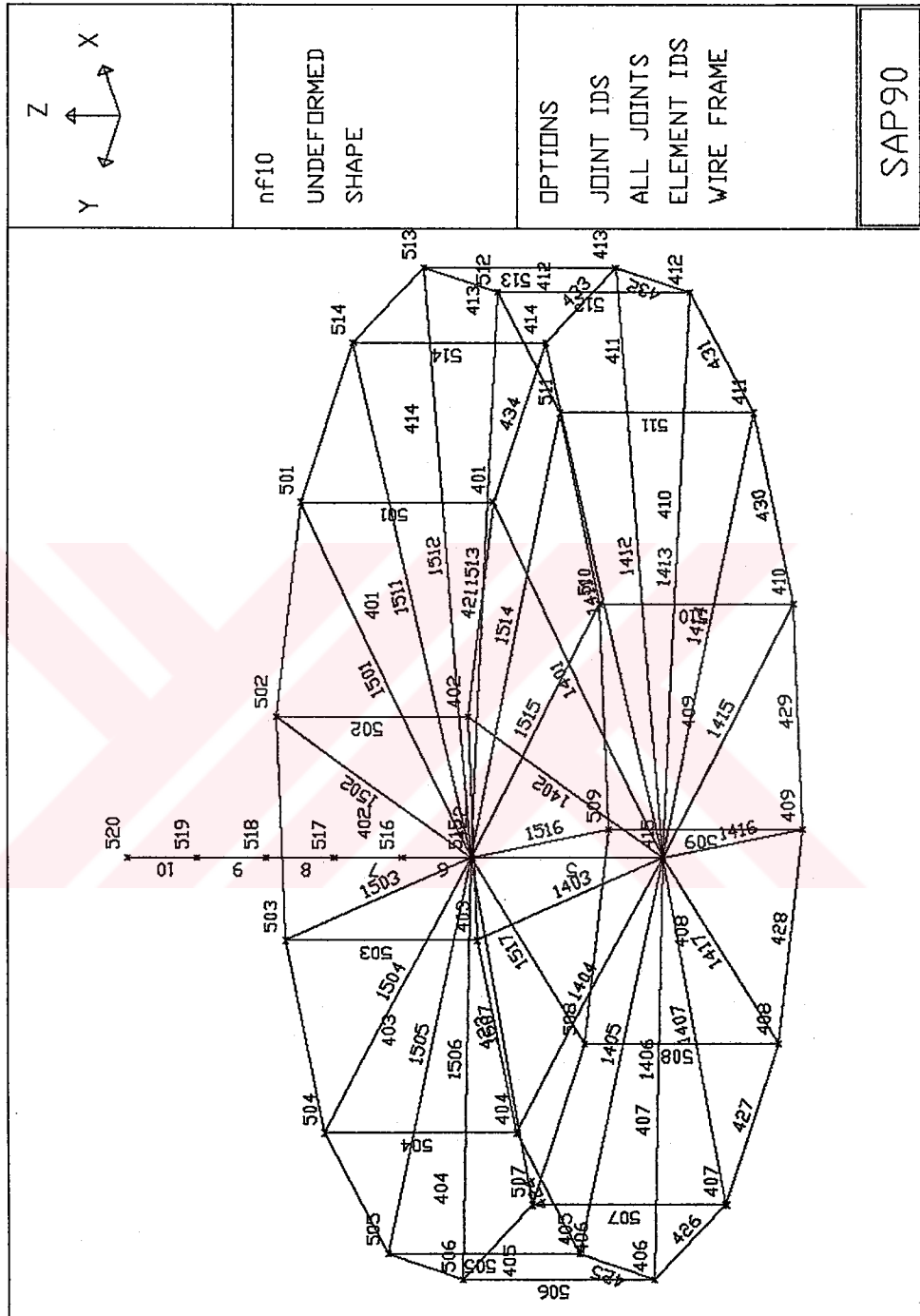


Figure 4.8 Model of the Structure between +10.00m ~ +20.00m Elevations

Showing Node and Element Numbering

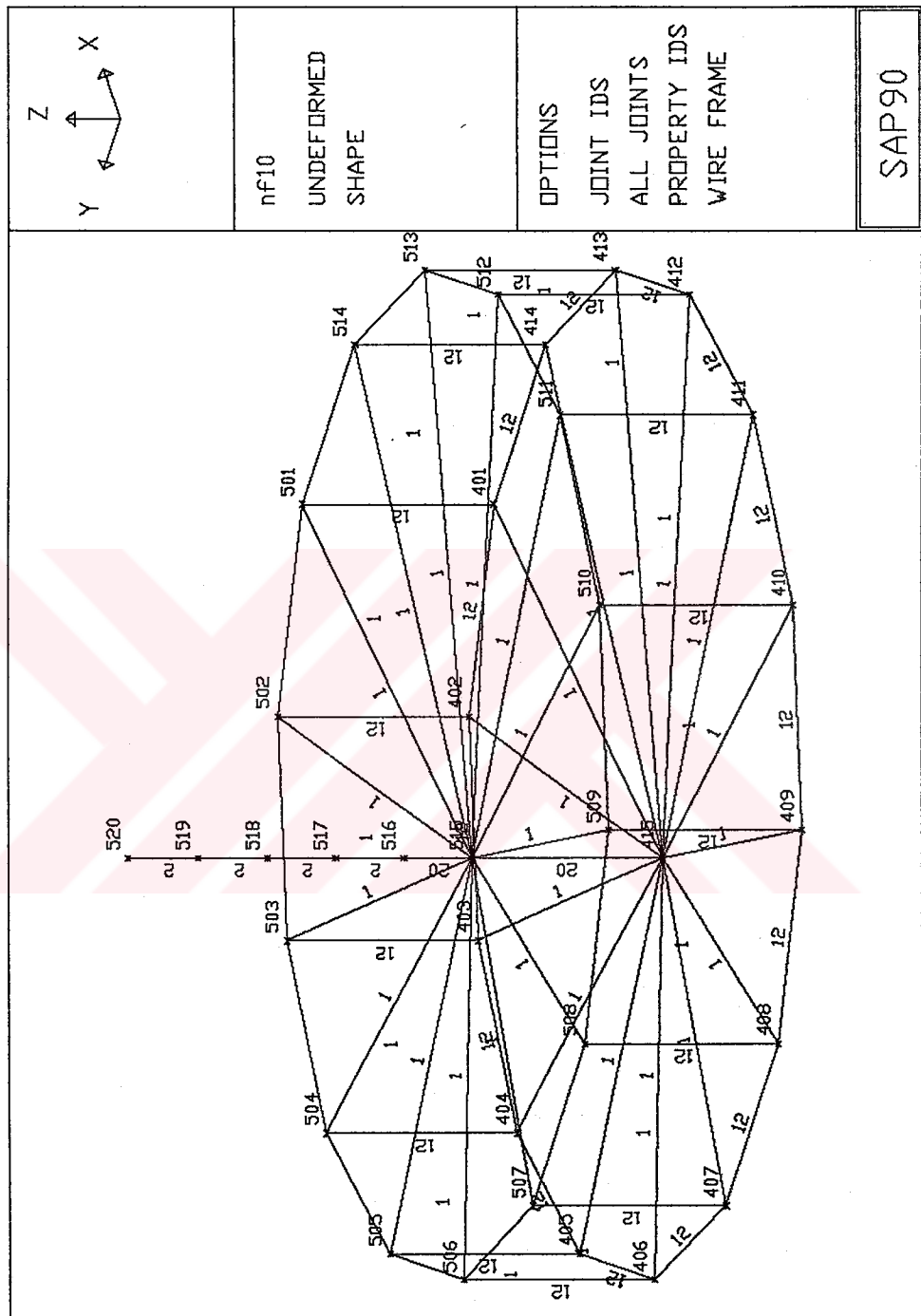


Figure 4.9 Model of the Structure between +10.00m ~ +20.00m Elevations

Showing Node and Element Section Property Numbering

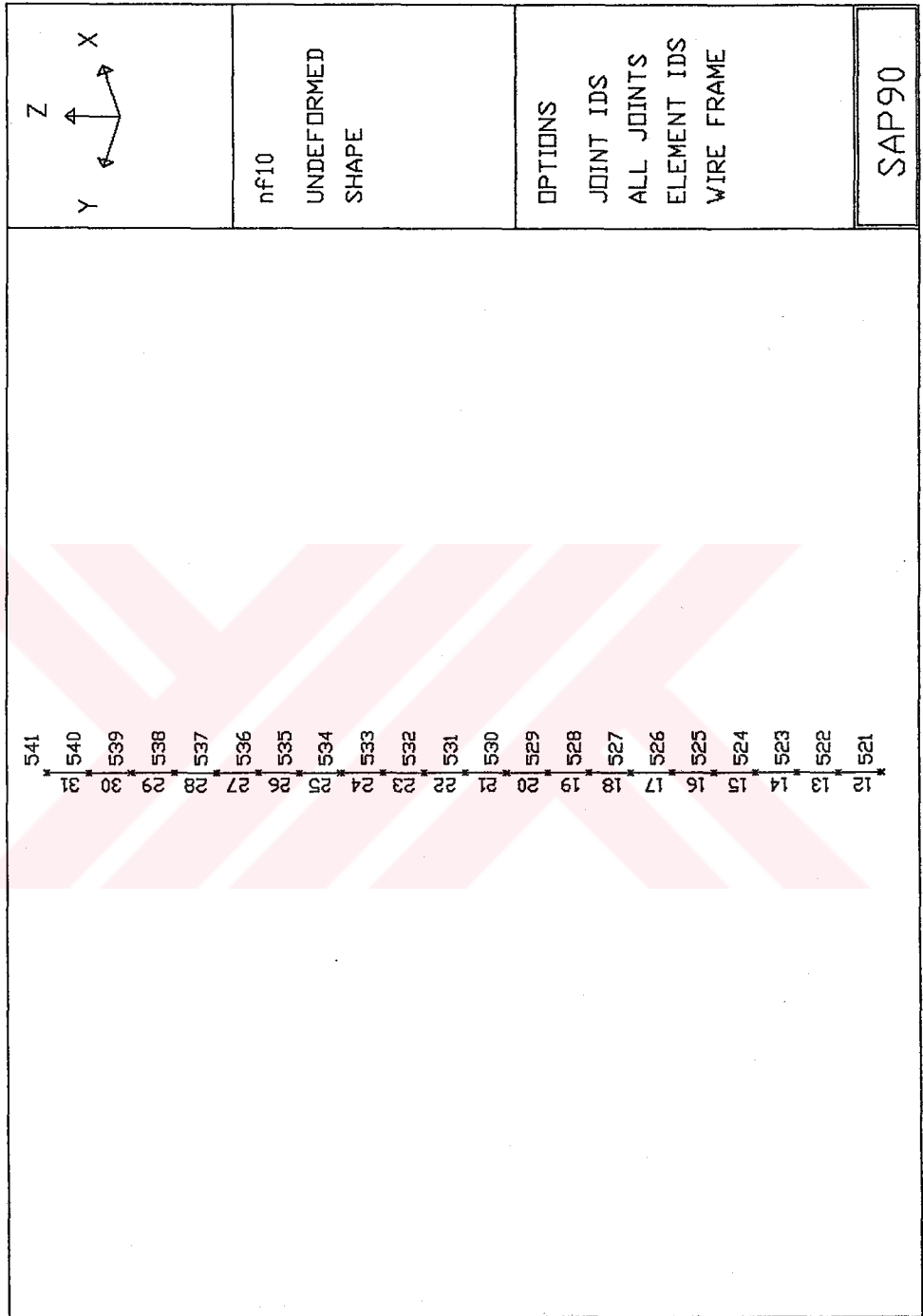


Figure 4.10 Model of the Structure between +20.00m ~ +40.00m Elevations
Showing Node and Element Numbering

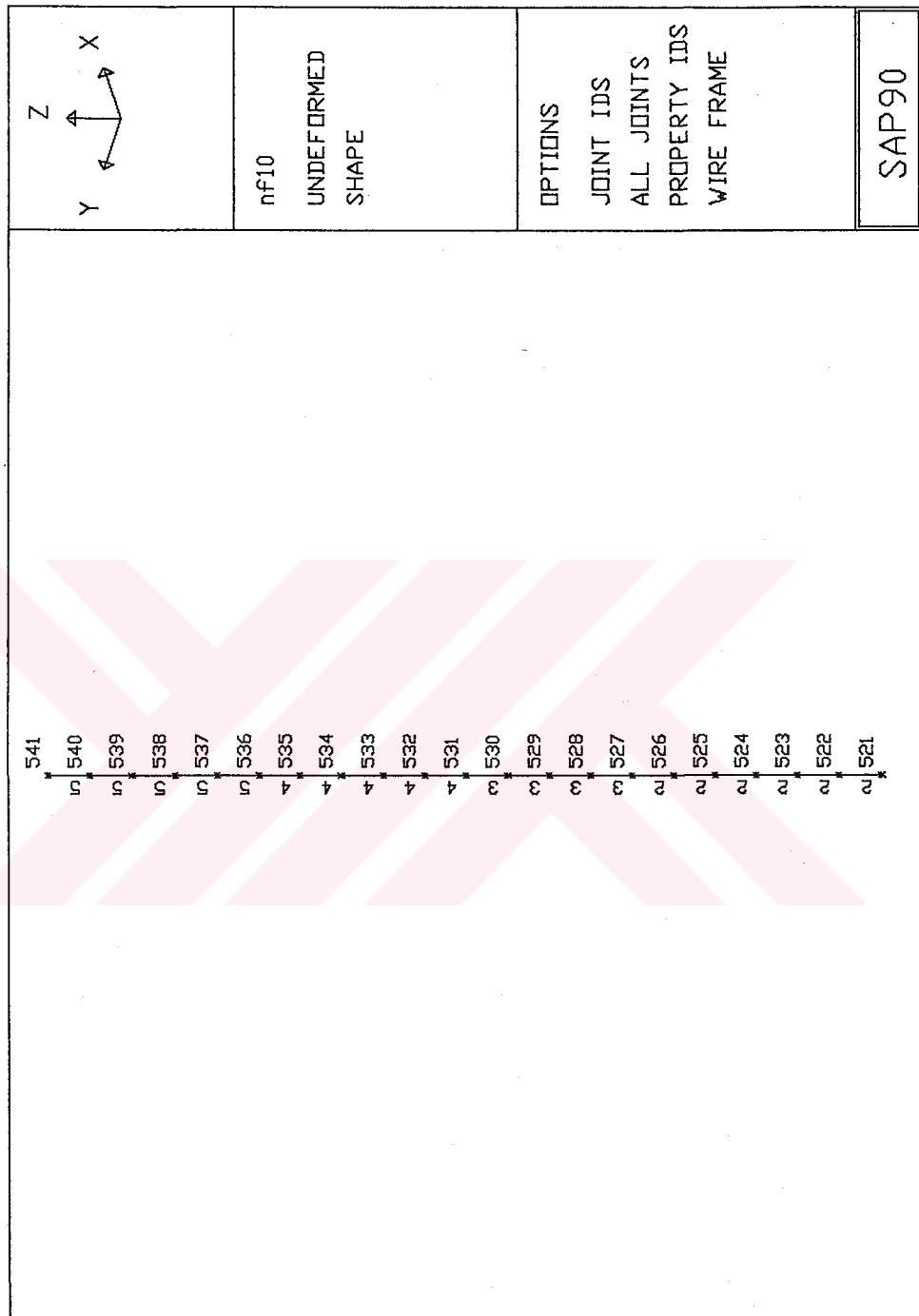


Figure 4.11 Model of the Structure between +20.00m ~ +40.00m Elevations

Showing Node and Element Section Property Numbering

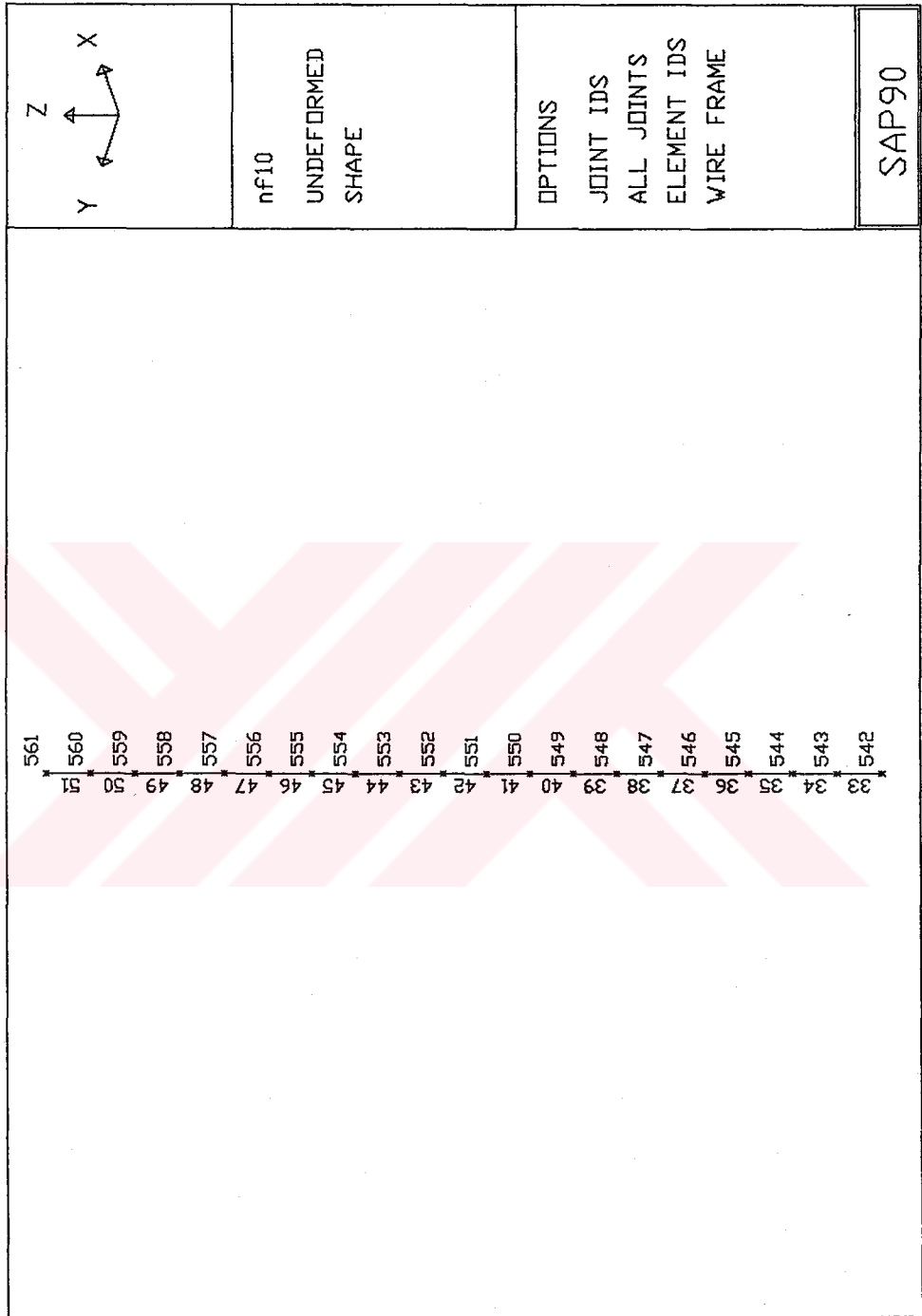


Figure 4.12 Model of the Structure between +40.00m ~ +60.00m Elevations
 Showing Node and Element Numbering

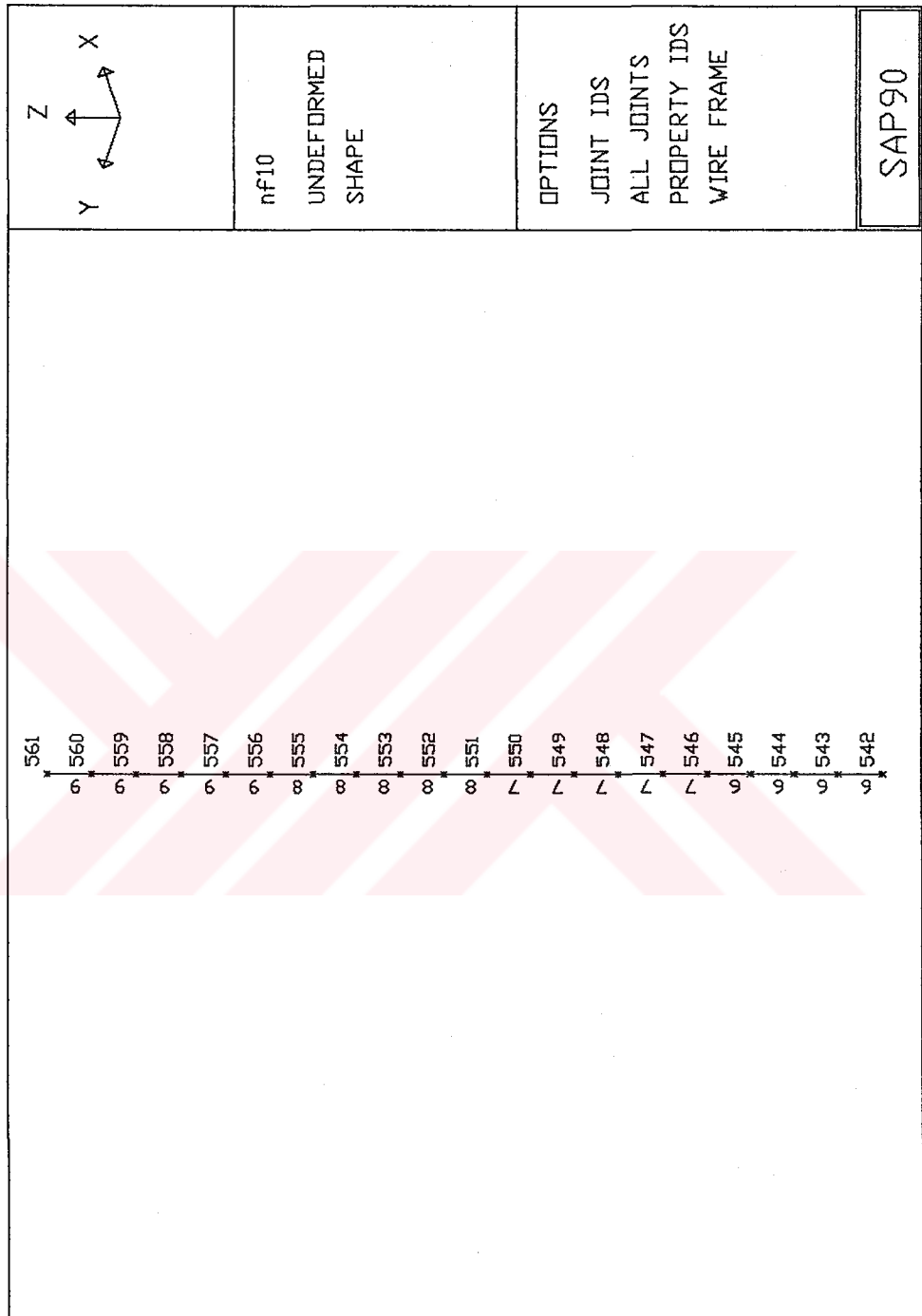


Figure 4.13 Model of the Structure between +40.00m ~ +60.00m Elevations

Showing Node and Element Section Property Numbering

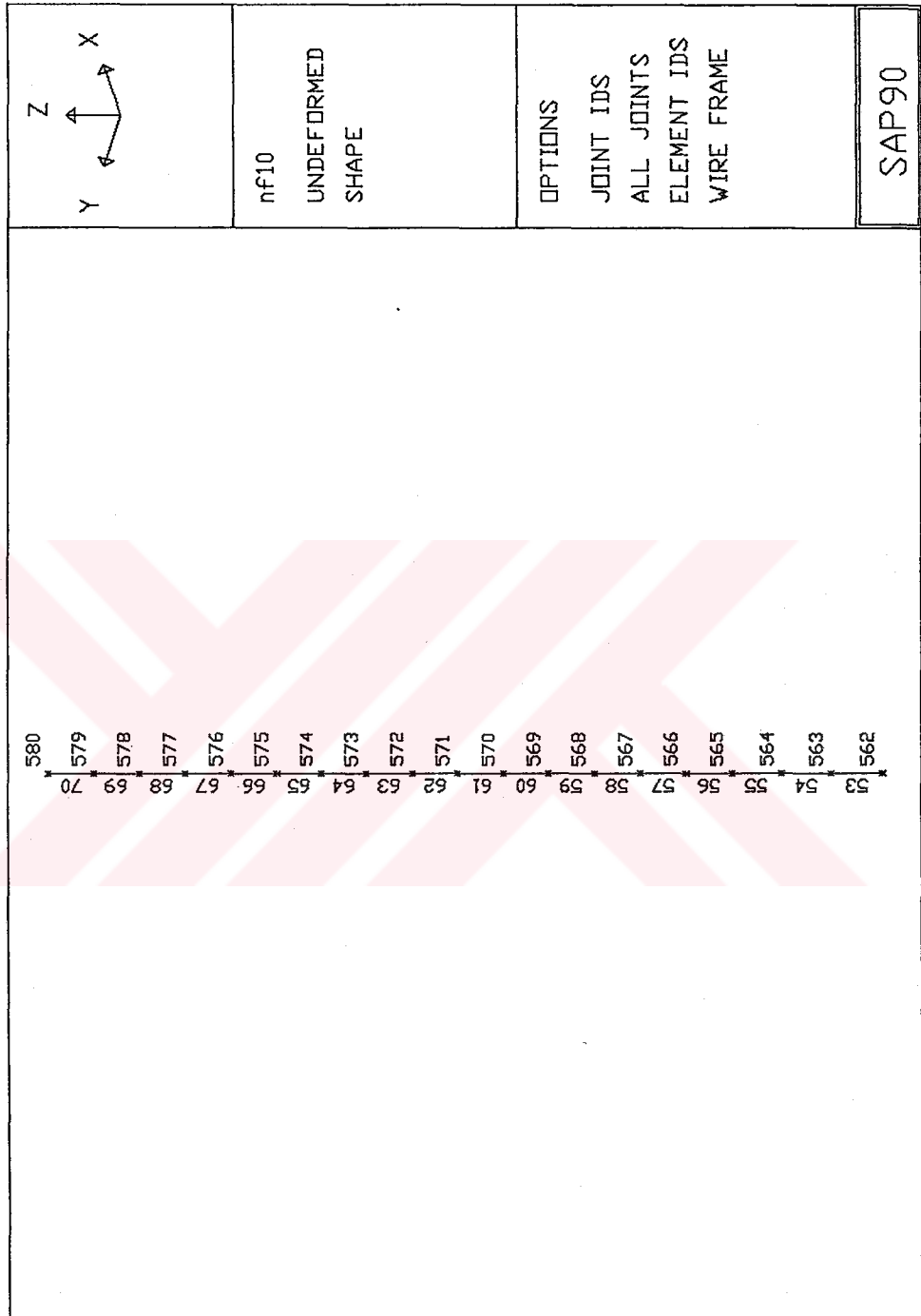


Figure 4.14 Model of the Structure between +60.00m ~ +80.00m Elevations
Showing Node and Element Numbering

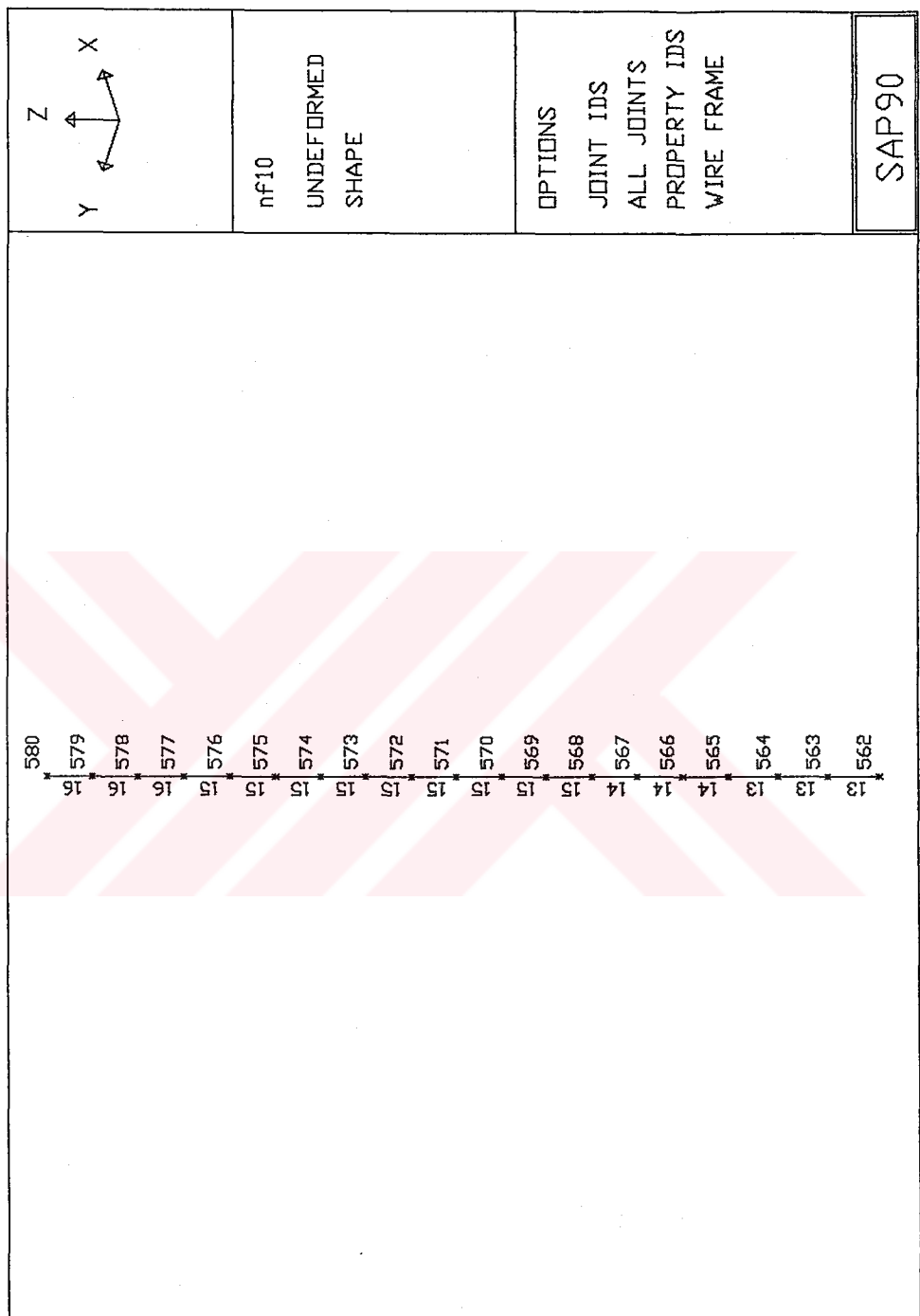


Figure 4.15 Model of the Structure between +60.00m ~ +80.00m Elevations

Showing Node and Element Section Property Numbering

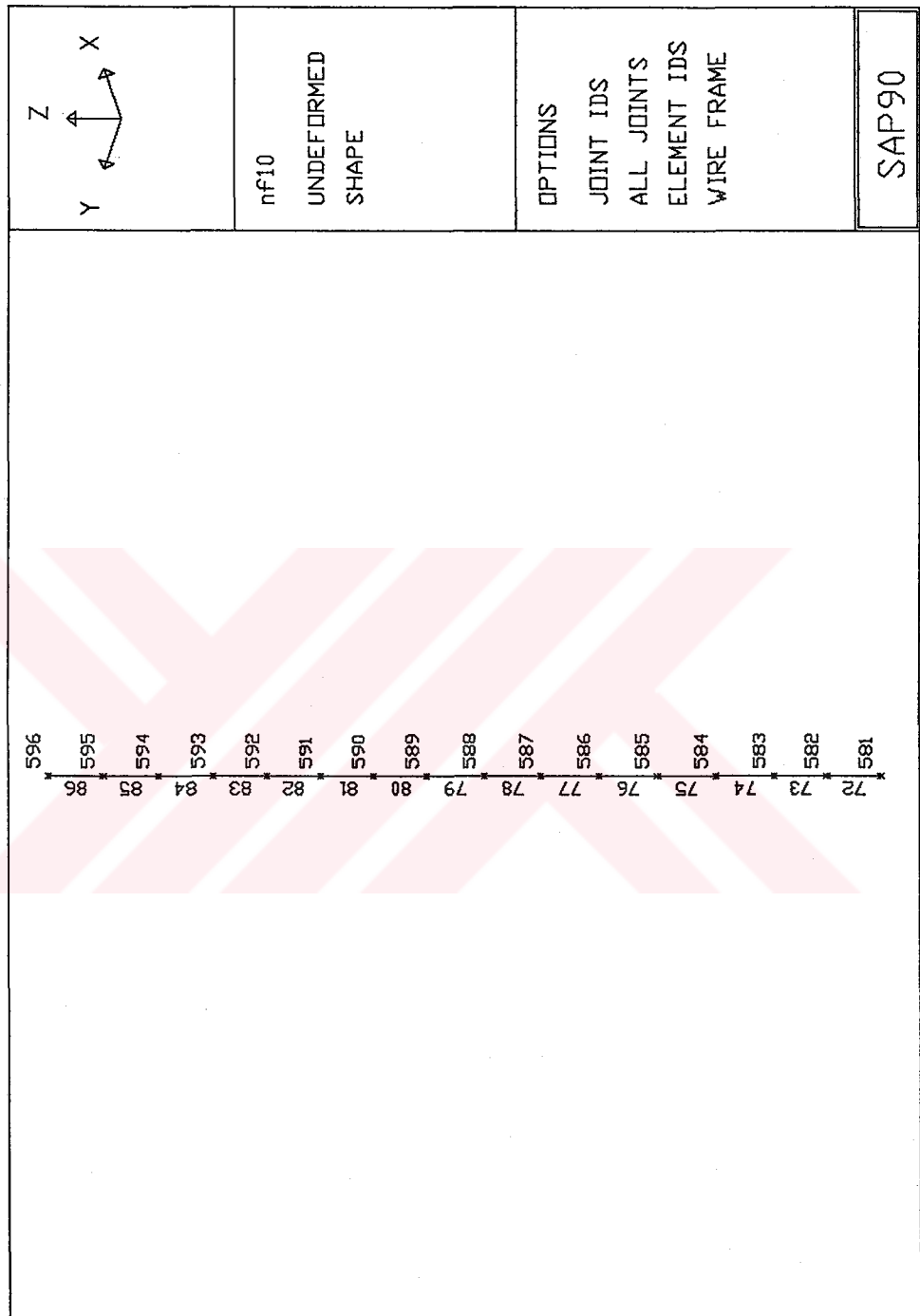


Figure 4.16 Model of the Structure between +80.00m ~ +96.00m Elevations

Showing Node and Element Numbering

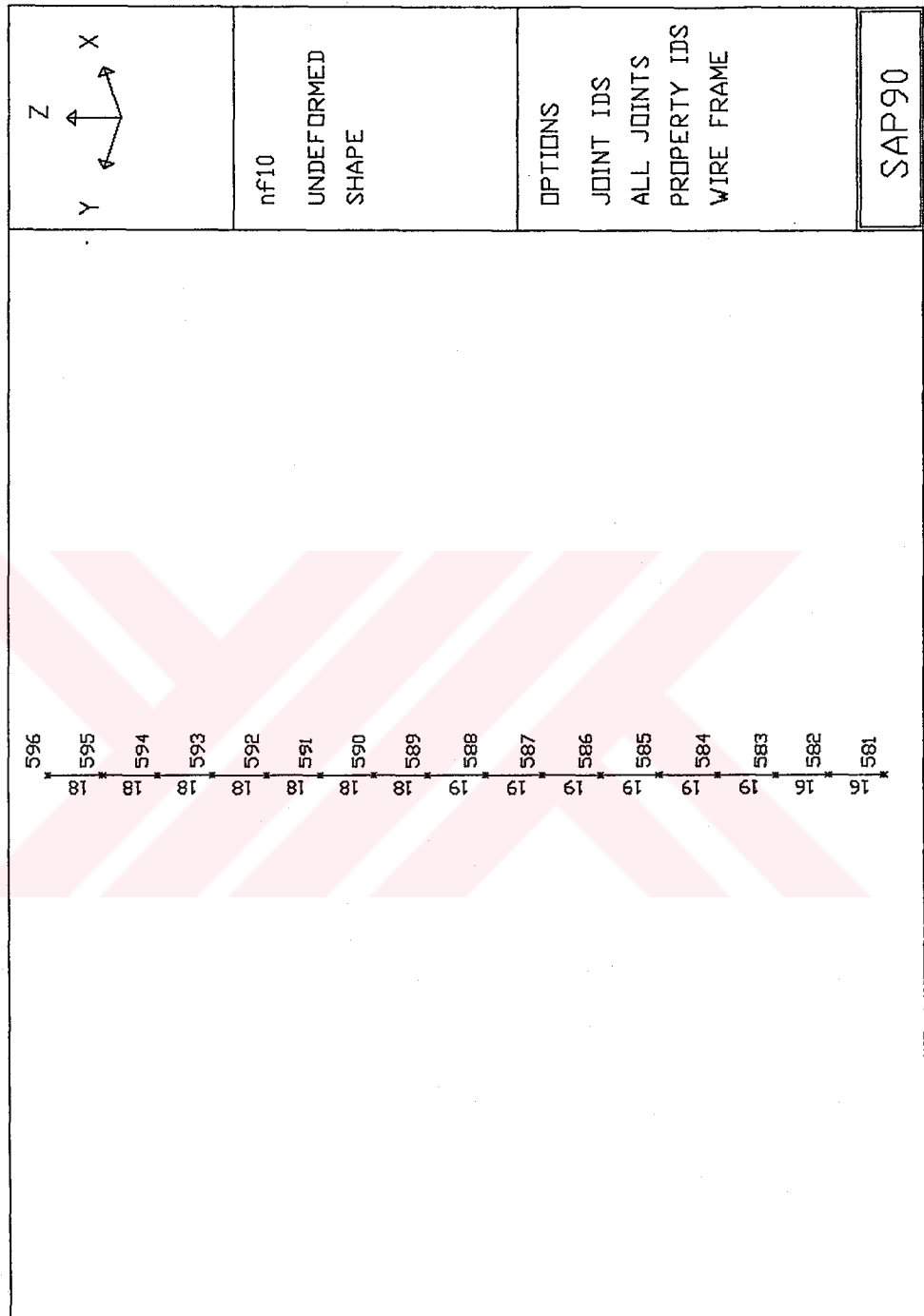


Figure 4.17 Model of the Structure between +80.00m ~ +96.00m Elevations

Showing Node and Element Section Property Numbering

4.2. Material and Element Properties

Model of the structure is defined as

- a. building section by skeleton and shell elements at every span
- b. tower section by one bar element between every story till +14.100m elevation and after +14.100m elevation by 1m long bar elements.

For different materials, 10 reinforced concrete, 1 steel and 1 GRP section properties are defined.

Reinforced Concrete:

$$\text{Modiolus of Elasticity} = 2.65 \times 10^6 \text{ t/m}^2 \text{ (TS500)}$$

$$\text{Weight per unit volume} = 2.500 \text{ t/m}^3 \text{ (TS500)}$$

Structural Steel:

$$\text{Modiolus of Elasticity} = 2.1 \times 10^7 \text{ t/m}^2$$

$$\text{Weight per unit volume} = 7.850 \text{ t/m}^3$$

Glass Reinforced Plastic:

$$\text{Modiolus of Elasticity} = 0.9 \times 10^5 \text{ t/m}^2 \text{ (ADC)}$$

$$\text{Weight per unit volume} = 0.200 \text{ t/m} \text{ (estimated from weight)}$$

Section #1 is used to define reinforced concrete floor beams.

$$b = 30 \text{ cm}, h = 50 \text{ cm}$$

$$A = 0.30 \times 0.50$$

$$= 0.150 \text{ m}^2$$

$$I_x = \frac{1}{12} 0.30 \times 0.50^3$$

$$= 0.003 \text{ m}^4$$

$$I_y = \frac{1}{12} 0.50 \times 0.30^3$$

$$= 0.001 \text{ m}^4$$

$$M = \{(0.150 + 1.50 \times 0.15) \times 2.500 + 0.200\} / 9.81$$

$$= 0.116 \text{ t/m}$$

Section #2 is used to define the tower structure reinforced concrete section between +0.000m and +26.00m elevations.

$$D = 4.50, t = 25 \text{ cm}$$

$$A = \left(\frac{3.14}{4}\right) (4.50^2 - 4.00^2)$$

$$= 3.336 \text{ m}^2$$

$$I = \frac{3.14}{64} (4.50^4 - 4.00^4)$$

$$= 7.559 \text{ m}^4$$

$$M = (3.336 \times 2.500) / 9.81$$

$$= 0.850 \text{ t/m}$$

Section #3 is used to define the reinforced concrete tower passing zone section between +26.00m and +30.00m elevations.

$$D = 4.50, t = 150\text{cm}$$

$$\begin{aligned} A &= \left(\frac{3.14}{4}\right) (4.50^2 - 1.50^2) \\ &= 14.130 \text{ m}^2 \end{aligned}$$

$$\begin{aligned} I &= \frac{3.14}{64} (4.50^4 - 1.50^4) \\ &= 19.870 \text{ m}^4 \end{aligned}$$

$$\begin{aligned} M &= (14.130 \times 2.500) / 9.81 \\ &= 3.432 \text{ t/m} \end{aligned}$$

Section #4 is used to define reinforced concrete tower section at +30.00m elevation.

$$D = 2.40, t = 45\text{cm}$$

$$\begin{aligned} A &= \left(\frac{3.14}{4}\right) (2.40^2 - 1.50^2) \\ &= 2.755 \text{ m}^2 \end{aligned}$$

$$\begin{aligned} I &= \frac{3.14}{64} (2.40^4 - 1.50^4) \\ &= 1.379 \text{ m}^4 \end{aligned}$$

$$\begin{aligned} M &= (2.755 \times 2.500) / 9.81 \\ &= 0.702 \text{ t/m} \end{aligned}$$

Section #9 is used to define reinforced concrete tower section at +60.90m elevation.

$$D = 2.40, t = 30\text{cm}$$

$$\begin{aligned} A &= \left(\frac{3.14}{4}\right) (2.40^2 - 1.80^2) \\ &= 1.978 \text{ m}^2 \end{aligned}$$

$$\begin{aligned} I &= \frac{3.14}{64} (2.40^4 - 1.80^4) \\ &= 1.113 \text{ m}^4 \end{aligned}$$

$$\begin{aligned} M &= (1.978 \times 2.500) / 9.81 \\ &= 0.504 \text{ t/m} \end{aligned}$$

(Section properties between #4 and #9 are defined by interpolating section properties #4 and #9. They are used for reinforced concrete sections between +30.00m and +60.90m elevations.)

Section #10 is used to define structural steel section at +60.90m elevation.

$$D = 1.20, t = 18\text{mm}$$

$$\begin{aligned} A &= \left(\frac{3.14}{4}\right) (1.20^2 - 1.164^2) \\ &= 0.067 \text{ m}^2 \end{aligned}$$

$$\begin{aligned} I &= \frac{3.14}{64} (1.20^4 - 1.164^4) \\ &= 0.187 \text{ m}^4 \end{aligned}$$

$$M = (0.067 \times 2.500 + 0.500) / 9.81$$

$$= 0.105 \text{ t/m}$$

Section #11 is used to define Glass Reinforced Plastic tower appendages.
(Section dimensions are taken from the report prepared by Alan Dick & Company Limited, Structural Analysis of Turkish Antenna GRP Cylinders)

$$D = 1.024\text{m} , d = 1.000\text{m}$$

$$A = \left(\frac{3.14}{4}\right) (1.024^2 - 1.000^2)$$

$$= 0.038 \text{ m}^2$$

$$I = \frac{3.14}{64} (1.024^4 - 1.000^4)$$

$$= 0.00013 \text{ m}^4$$

$$M = 0.200 / 9.81$$

$$= 0.020 \text{ t/m}$$

(GRP antenna weight is assumed as 200 kg/m)

Section #12 is used to define dummy reinforced concrete beams and columns. $b_w = 20\text{cm} , d = 20\text{cm}$

$$A = 0.20 \times 0.20$$

$$= 0.040 \text{ m}^2$$

$$I_x = I_y = \frac{1}{12} 0.20 \times 0.20^3$$

$$= 0.0001333 \text{ m}^4$$

Shell elements are used to define the reinforced concrete thin shear walls at outer sides of the building part of the structure.

$$t = 20 \text{ cm}$$

$$\begin{aligned} M &= (0.20 \times 2.500) / 9.81 \\ &= 0.051 \text{ t/m}^2 \end{aligned}$$

4.3. Previous Investigations

Measurement of structural response to the ambient excitations is one of the best methods utilized to assess the dynamic characteristics of such massive structures so the dynamic characteristics of the Kars TV Antenna Structure have been measured to compare the results with mathematical model.

The peak frequencies observed on the Fourier Amplitude spectra are shown to be directly related to the modal frequencies of vibration of the structure. The first four modal frequencies of vibration are determined to be 0.55, 1.28, 2.25 and 3.24 Hz. The first four mode shapes, based on the amplitude ratios indicated above, are illustrated in Figures 4.18, 4.19, 4.20, and 4.21 where the lines indicate the modal shape in direction perpendicular to the internal stair case, and the dashed lines indicate the modal shape in direction parallel to internal stair case. Due to the specific mass and stiffness distribution of the tower structure the ratio

of the modal amplitudes at the 10th and 90th meter elevations of the tower for the first mode is in the vicinity of 100.

4.4. Evaluation of Results

The tower is described in the X-Y-Z space, z axis being the axis along the corresponding mode shapes have been obtained. For each mode, two results are obtained: first for the mode in the X-Z plane and the other in the Y-Z plane. Due to the fact that the structure has similar characteristics in both planes, the results are similar and there is no reason to present two similar modes. Therefore, only the odd modes are presented.

The natural frequencies and periods obtained from the finite element model and those obtained experimentally are given in Table 4.1. The corresponding mode shapes are given in Figs. 4.18, 4.19, 4.20 and 4.21. A study of Table 4.1 reveals that the experimentally obtained natural frequencies and those obtained from the finite element model are in very satisfactory agreement. Especially the results for the first and second modes are almost the same. The discrepancy between experimental and numerical results increases as the mode number increases but this is expected at higher modes.

The agreement between the experimental and numerical results assures the verification of the finite element model. Thus, having gained confidence in the finite element model, dynamic analysis of the tower can be applied in both time and frequency domain.

Table 4.1 Numerical and Experimental Natural Frequencies and Periods

| Mode | Experimental | | Finite Element Model | |
|------|--------------|-----------|----------------------|-----------|
| | Freq.(Hz) | Period(s) | Freq.(Hz) | Period(s) |
| 1 | 0.55 | 1.818 | 0.556 | 1.799 |
| 2 | 1.28 | 0.781 | 1.260 | 0.794 |
| 3 | 2.25 | 0.444 | 2.087 | 0.479 |
| 4 | 3.24 | 0.309 | 3.451 | 0.290 |

4.5 Time Domain Analysis

For the near field earthquake analysis, an earthquake at an epicentral distance of 15 km, having a Peak Ground Acceleration (PGA) level of 0.3g at the bedrock level and 0.38g at the soil surface corresponding to a magnitude of $M_s=6.0$ was considered. On the other hand, for the far field earthquake analysis, an earthquake at an epicentral distance of 90 km, having a PGA level of 0.05g at the bedrock level and 0.11g at the soil surface corresponding to a magnitude $M_s=7.0$ was taken into account.

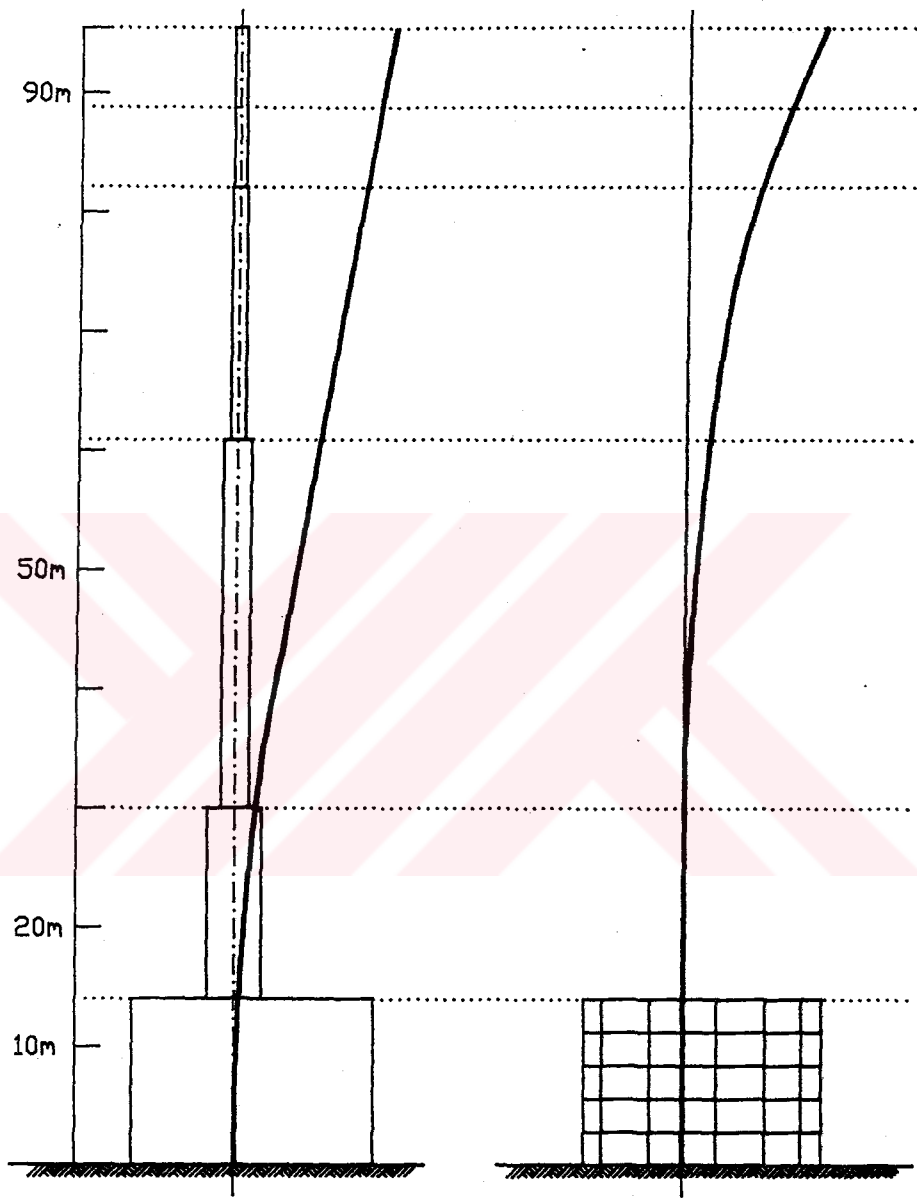


Figure 4.18 First Vibration Mode Shapes

Left : Ambient Vibration Test , $F=0.55$ Hz

Right : Dynamic Analysis by Computer , $F=0.556$ Hz

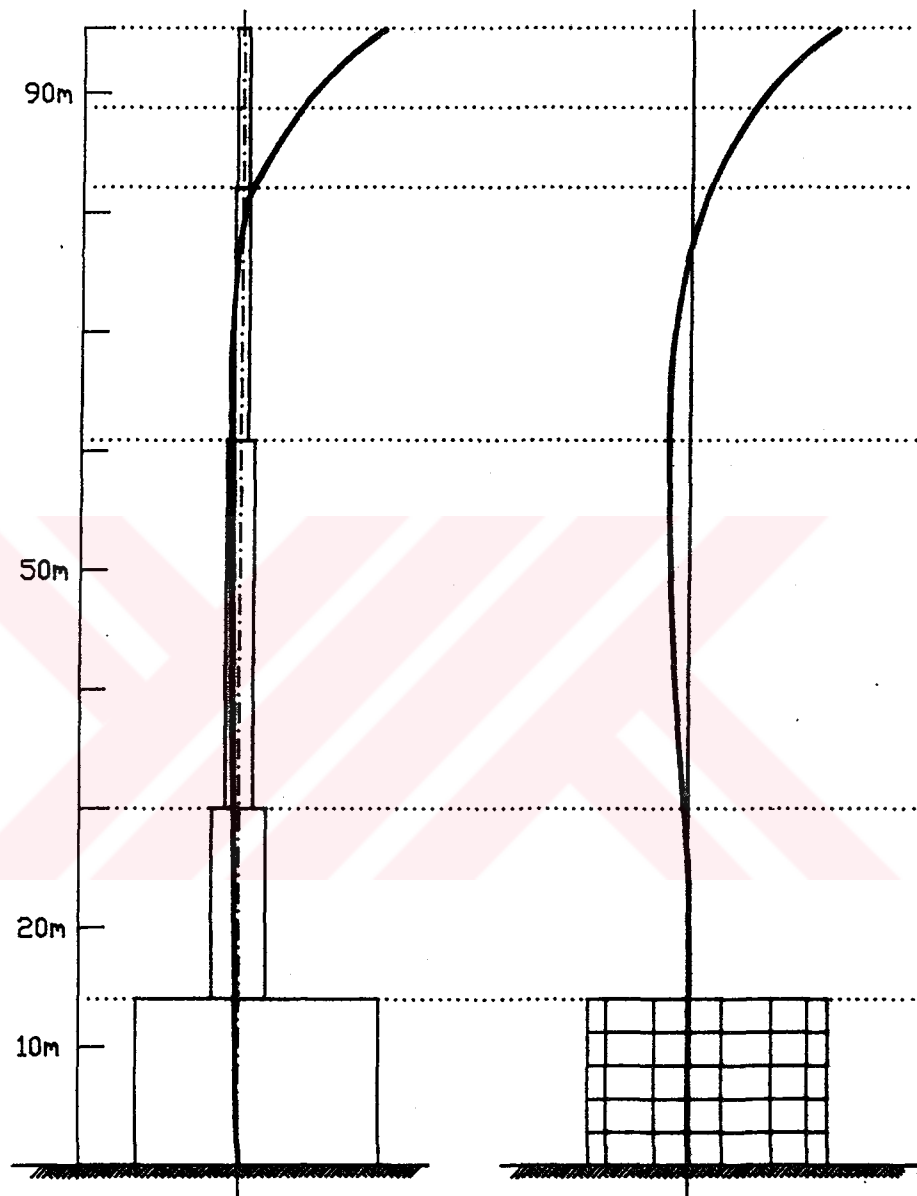


Figure 4.19 Second Vibration Mode Shapes

Left : Ambient Vibration Test , $F=1.28$ Hz

Right : Dynamic Analysis by Computer , $F=1.260$ Hz

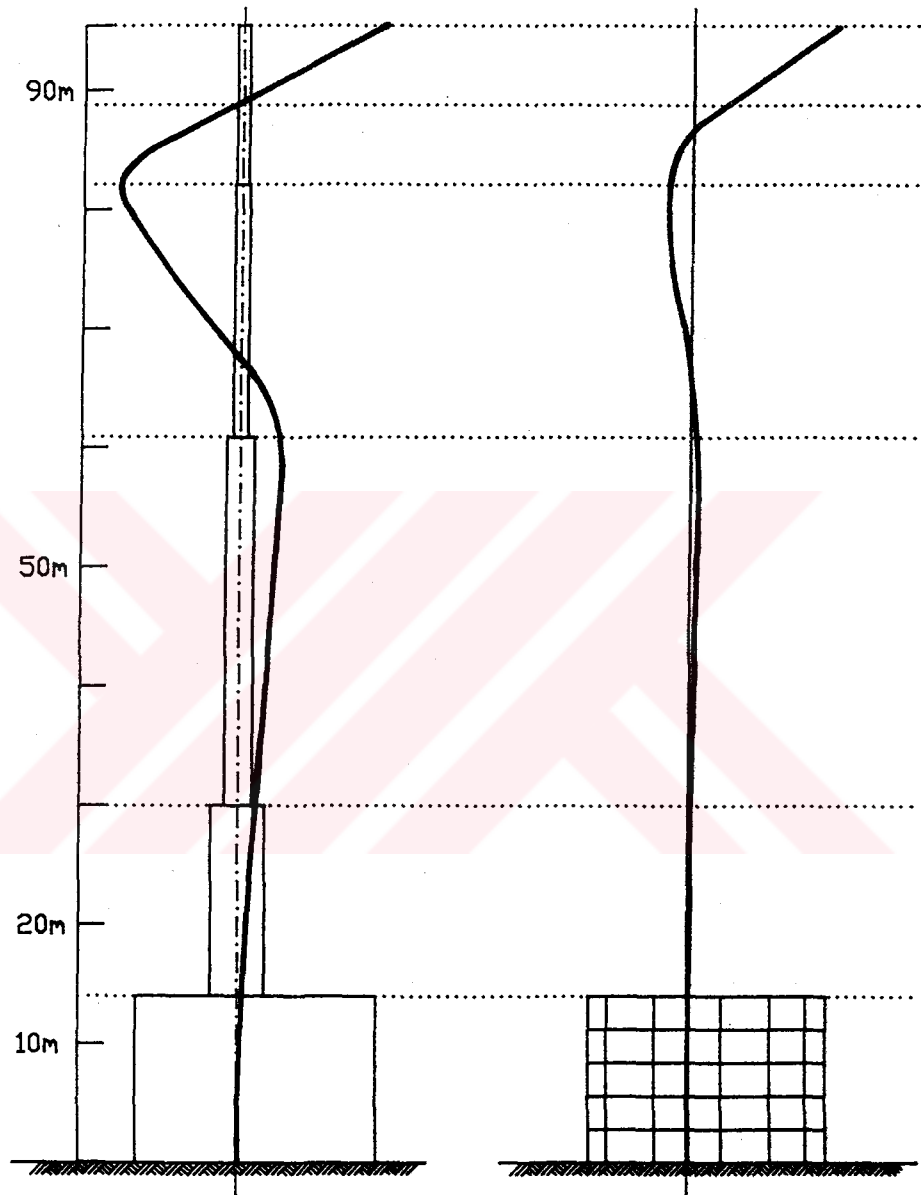


Figure 4.20 Third Vibration Mode Shapes

Left : Ambient Vibration Test , $F=2.25$ Hz

Right : Dynamic Analysis by Computer , $F=2.087$ Hz

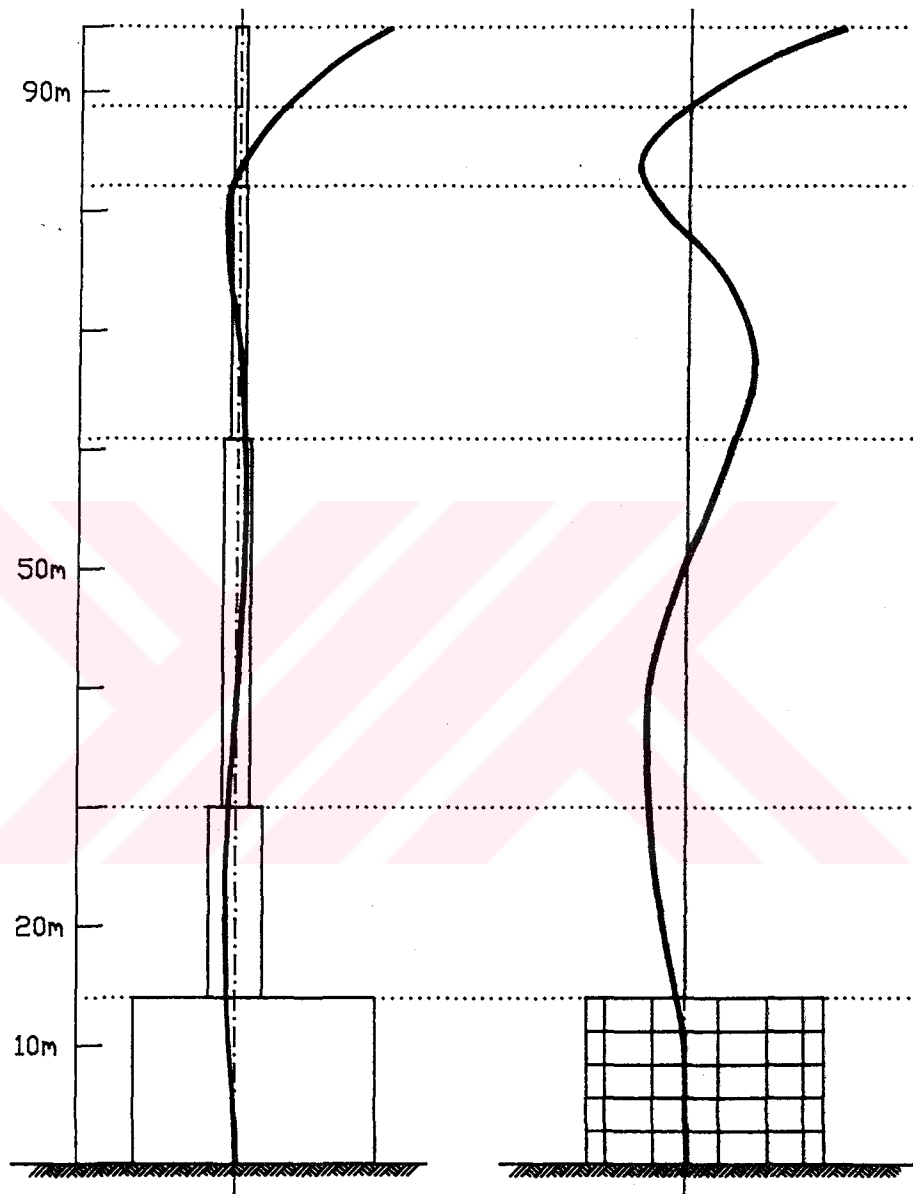


Figure 4.21 Fourth Vibration Mode Shapes

Left : Ambient Vibration Test , $F=3.24$ Hz

Right : Dynamic Analysis by Computer , $F=3.451$ Hz

As the observed damage on the structure, it seems to be caused by Spitak (Armenian) earthquake, which is a far field earthquake, only far field earthquake case is observed for time domain analysis.

The acceleration function acting at the base of the tower is given in Figure 4.22. As given before, the maximum acceleration is 0.11g as seen in the figure. The same acceleration function, but now with m/sec^2 units, is shown in Figure 4.23.

There different structural damping values are used in the numerical analysis. They are 0.01, 0.02 and 0.05. It should be noted that low strain levels in the tower are expected to generate low damping. Far field earthquakes, especially the one considered in the present work, are expected to cause low strain levels. A damping value of 0.01 encompasses low strain levels and, at the other end, a damping value of 0.05 is handled. The maximum acceleration, displacement, moment and shear force at the bottom of the GRP section of the tower are given in Table 5.2 for damping values of 0.01, 0.02 and 0.05.

Following figures show the acceleration, displacement, moment, shear force as function of time for the node and the element at the bottom of the GRP section of the tower, for the damping values of 1%, 2% and 5%, respectively for

the node.

Table 4.2 Maxima for Different Damping Values

| Damping | 1% | 2% | 5% |
|--|-------|-------|--------|
| Max. Acceleration (m/s ²) | 11.63 | 8.63 | 5.36 |
| Max. Displacement (m) | 0.129 | 0.104 | 0.0717 |
| M _{max} (t.m) | 62.45 | 51.53 | 32.05 |
| V _{max} (t) | 5.324 | - | - |

Damping value of 1% is more realistic for the present case since the far field earthquake under consideration is expected to cause low strain levels corresponding to the activation of low damping values. Figure 5.28, 5.29, and 5.30 gives the acceleration as a function of time at the midpoint (nodal point 590), top (nodal point 596) of the GRP section and displacement at the top of GRP section. Maximum acceleration is 18.54 m/s² at the midpoint, 65.80 m/s² at the top and maximum displacement is 0.485m at the top.

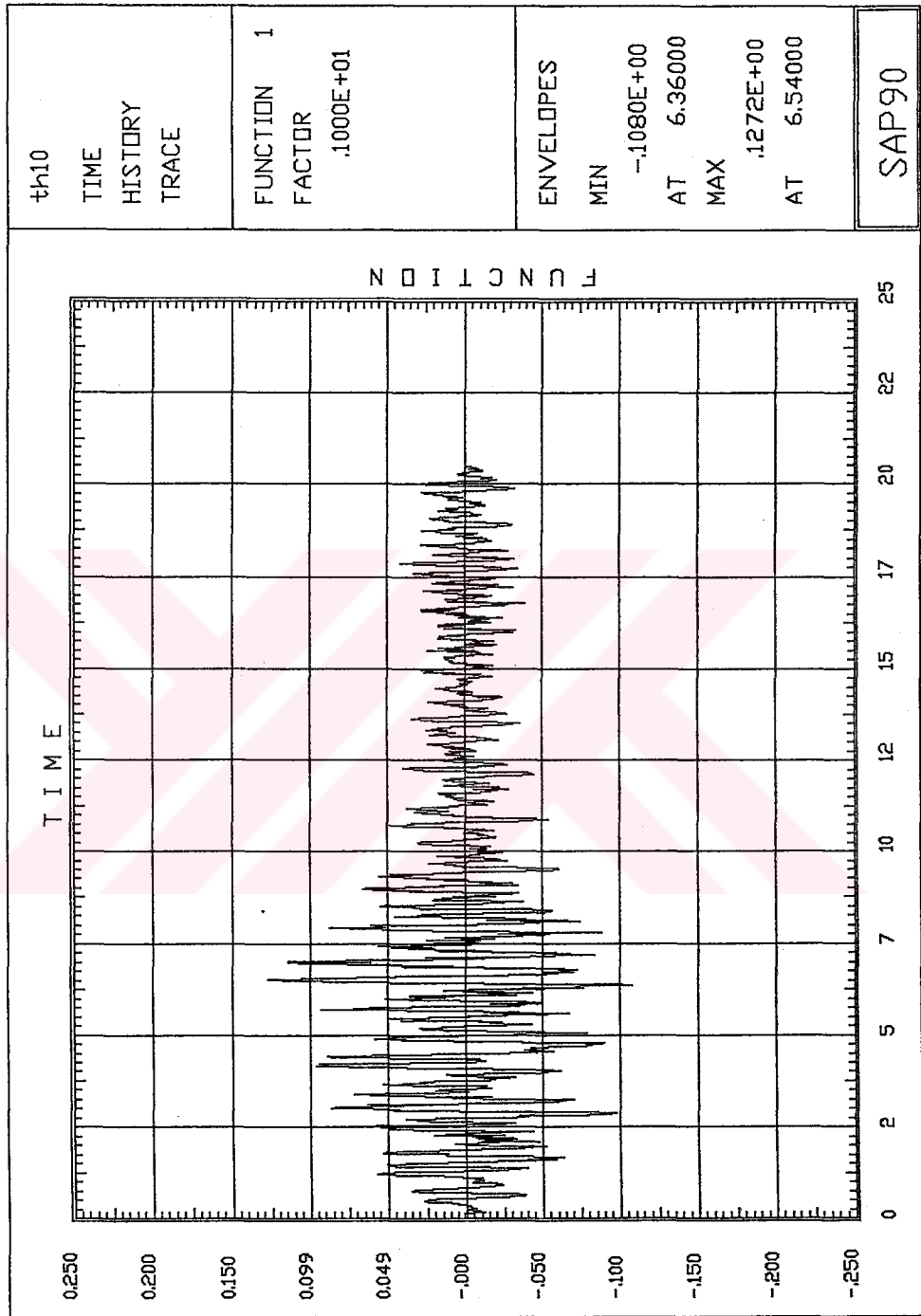


Figure 4.22 Time History Function of Computer Model versus Time

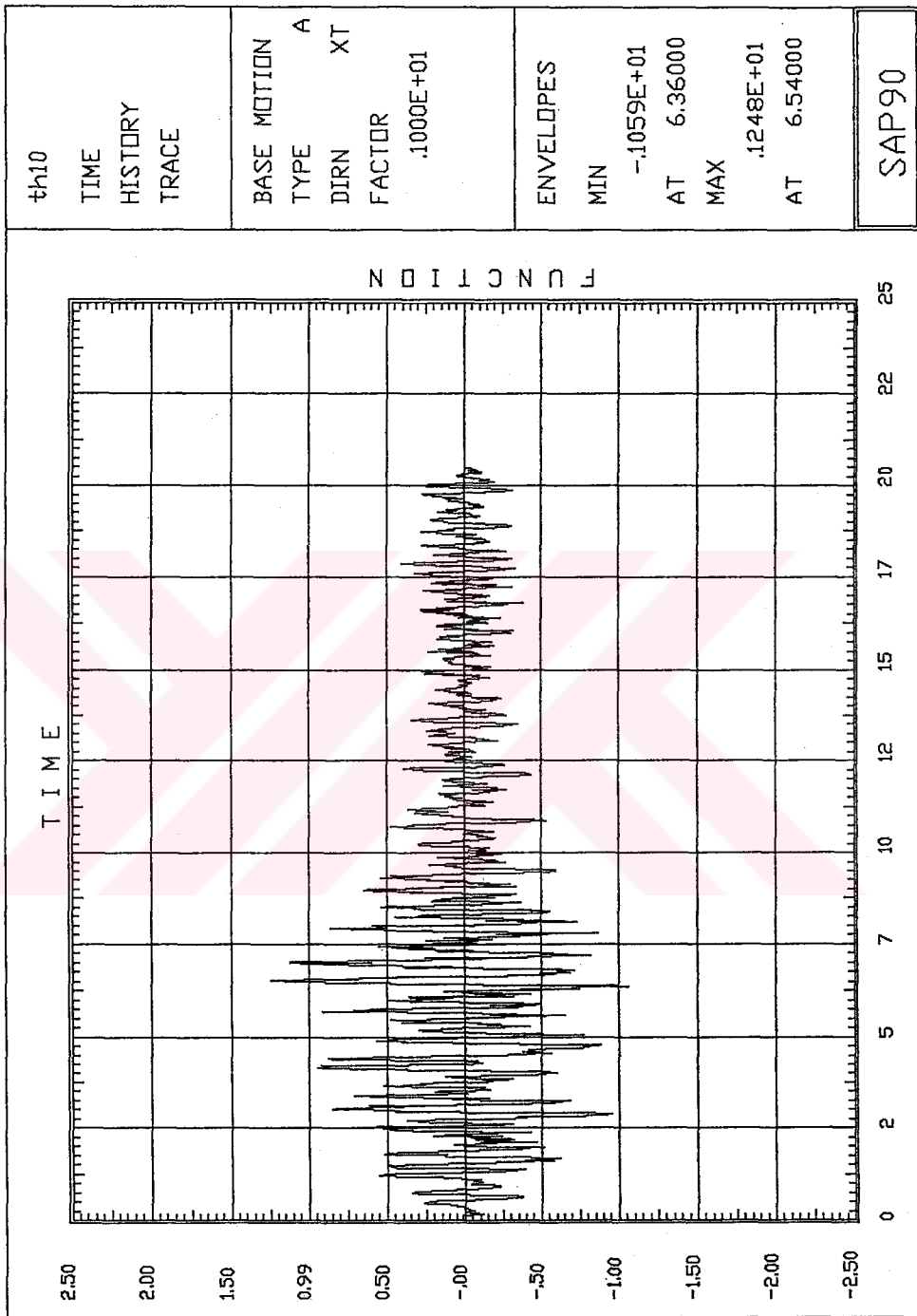


Figure 4.23 Base Acceleration at XT Direction versus Time

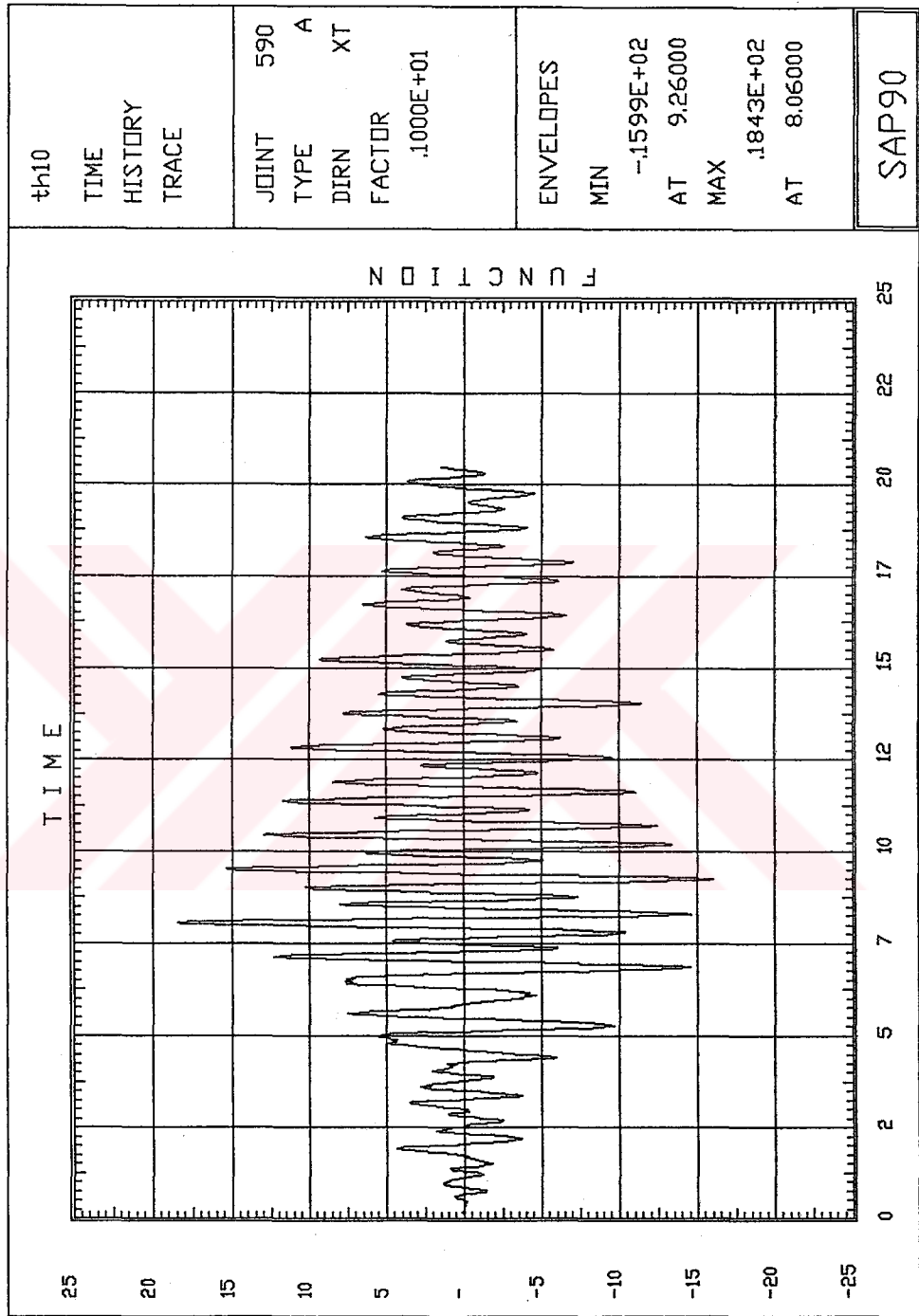


Figure 4.24 Acceleration of Node 590 at XT Direction versus Time

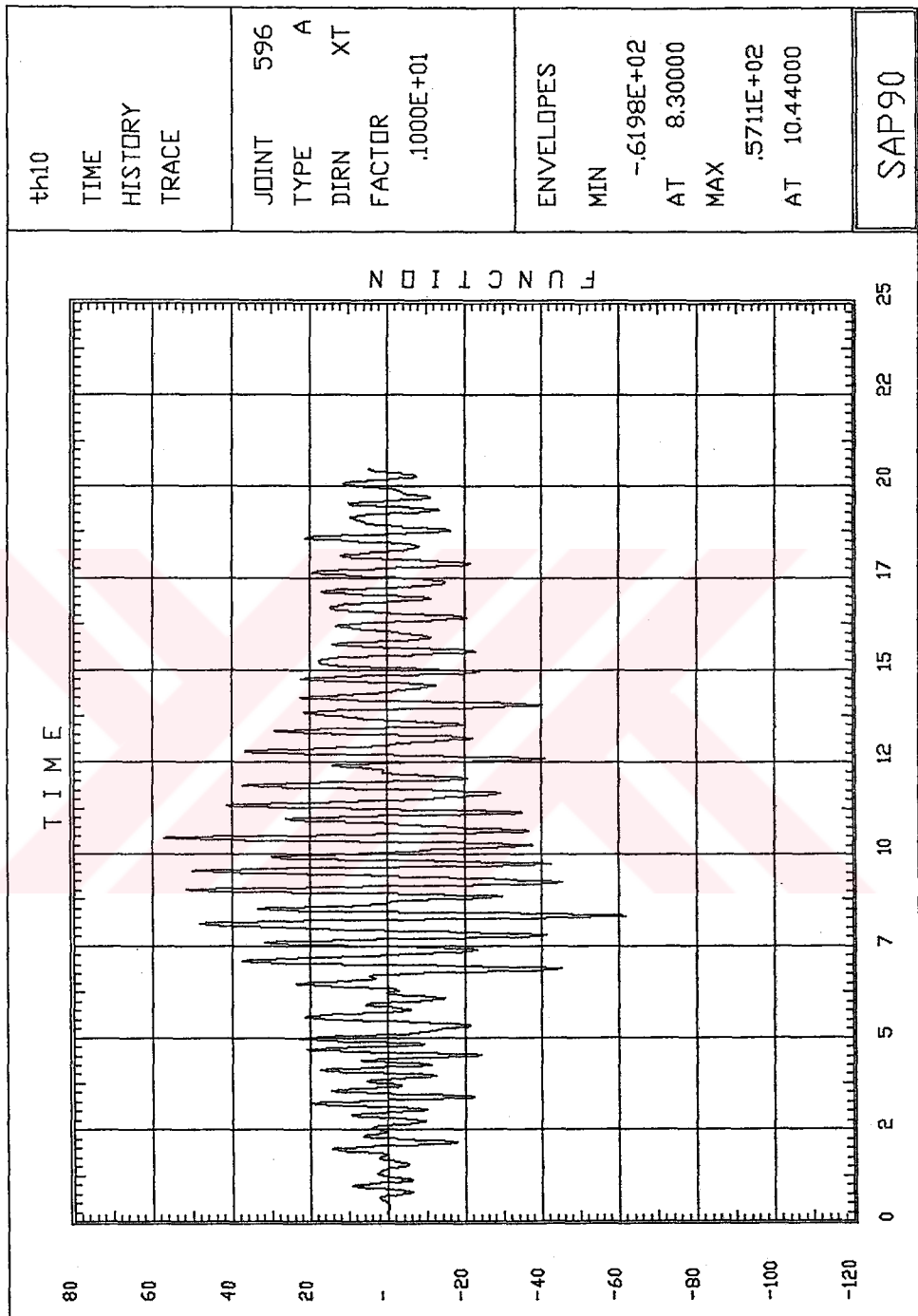


Figure 4.25 Acceleration of Node 596 at XT Direction versus Time

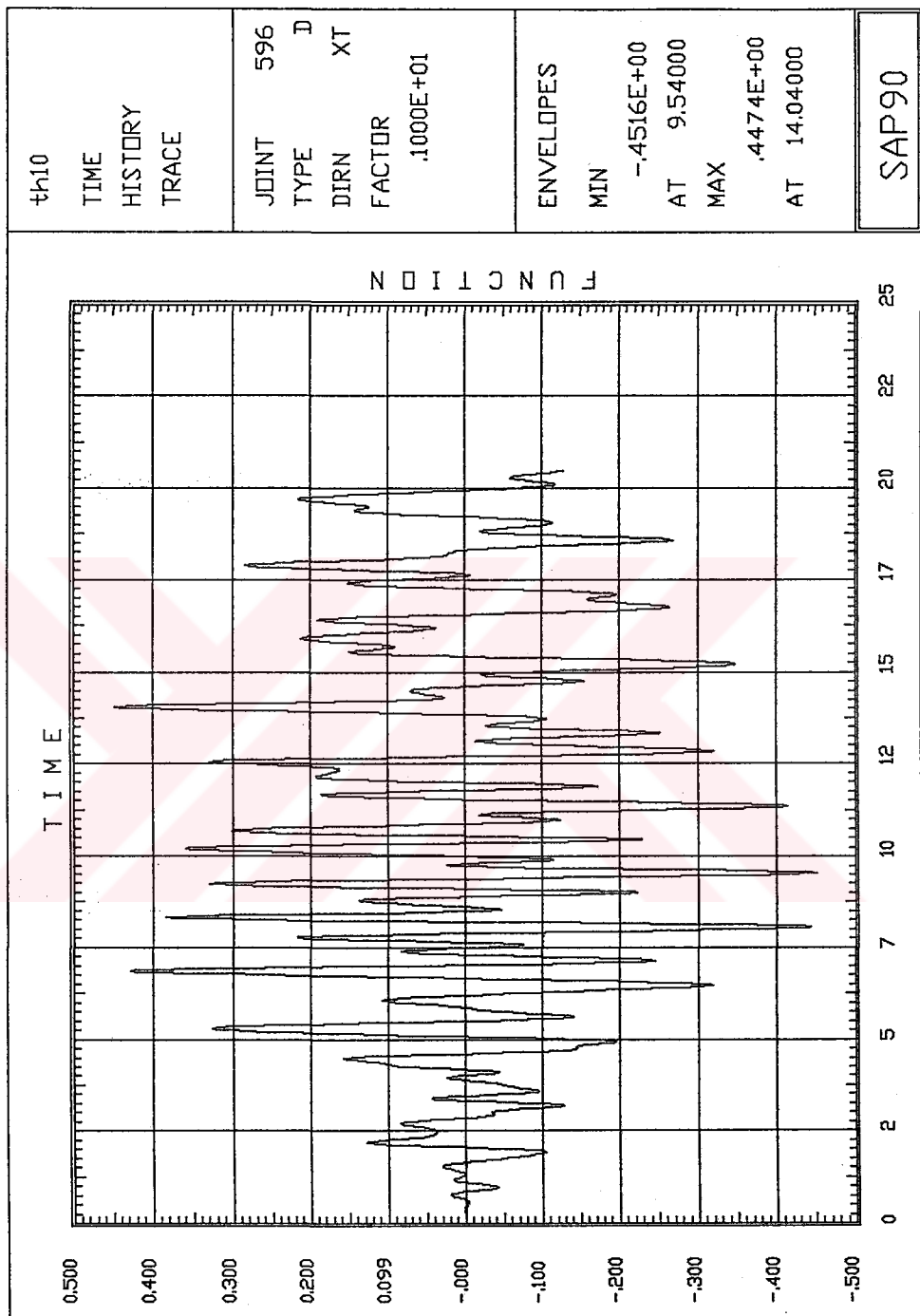


Figure 4.26 Displacement of Node 596 at XT Direction versus Time

The values obtained from the numerical analysis in the time domain should be verified with those obtained in the frequency domain. This requires response spectrum analysis which is presented in the following section.

4.6. Response Spectrum Analysis

For the near field earthquake analysis, an earthquake at an epicentral distance of 15 km, having a Peak Ground Acceleration (PGA) level of 0.3g at the bedrock level and 0.38g at the soil surface corresponding to a magnitude of 15km was considered. On the other hand, for the far field earthquake analysis, an earthquake at an epicentral distance of 90 km, having a PGA level of 0.05g at the bedrock level and 0.11g at the soil surface corresponding to a magnitude $M_s=7.0$ was considered.

In the response spectrum analysis, it is necessary to provide the deterministic design basis response spectra for both the near field (PGA=0.38g) and far field (PGA=0.11g) events. These spectra are obtained following the ATC 3-06 spectral shapes using a site factor of $S=1$ by another team. The ATC 3-06 type spectra corresponding to the near and far-field events are provided in following figures for 1%, 2%, and 5% damping respectively.

The empirical regression equations developed by Joyner and Boore can be utilized for the frequency domain simulation of the earthquake ground motion at the site. This regression analysis provides the spectral amplitudes with respect to earthquake magnitude, epicentral distance and the site conditions at selected frequencies. These empirical spectra, obtained for the near field and the far field events, have been compared with those provided in Figures 4.27 and 4.28 and it has been determined that ATC 3-06 based spectra provide prudent level of conservatism to be utilized as the design basis response spectra.

The response spectra provided are for the horizontal component of the ground motion and for a relative viscous damping ratio of 5%. The vertical spectra for the same can be computed by multiplying the horizontal spectral ordinates by $2/3$ following the USBRC and IAEA criteria. On the basis of the same criteria, the following factors can be used to multiply the spectral ordinates of the spectrum with 5% damping to obtain the spectrum for other damping factors:

Table 4.3 Spectral Adjustment Factors for Damping

| | | | | | | | |
|-------------------|------|------|------|------|------|------|------|
| Damping Ratio (%) | 1 | 2 | 5 | 7 | 10 | 15 | 20 |
| Factor | 2.00 | 1.25 | 1.00 | 0.90 | 0.80 | 0.70 | 0.60 |

The response spectra obtained as described above are now used in

SAP90 to determine the deformed shape, moment distribution and shear distribution along the GRP section of the tower.

The maximum displacement occurs at the top of the GRP section. Maximum moment and shear are at element number 74 which is at the bottom of the GRP section.

Table 4.4 Maxima Obtained from the Response Spectrum Analysis

| | Near field | | | Far field | | |
|-----------------------|------------|-------|-------|-----------|-------|-------|
| Damping | 0.01 | 0.02 | 0.05 | 0.01 | 0.02 | 0.05 |
| Max. Displacement (m) | 1.34 | 0.89 | 0.70 | 0.47 | 0.31 | 0.24 |
| M_{\max} (t.m) | 130.90 | 88.95 | 69.81 | 38.19 | 25.95 | 20.37 |
| V_{\max} (t) | 13.01 | 8.79 | 6.91 | 3.81 | 2.57 | 2.02 |

4.7. Discussion

The maximum moment occurring at the bottom of the GRP section of the tower has been obtained by various approaches. The fact that either one of the near and far field earthquakes may be critical has been taken into consideration. The fact that the damping value may play a critical role in the design process has been taken into consideration. Both time domain and response spectrum analyses

have been carried out to verify the results. The maximum moments occurring at the bottom of the GRP section of the tower have been obtained for all possible combinations of the parameters mentioned and the results are summarized in Table 5.5. It is concluded that, for this structure for far field analysis, a damping value of 1% should be used. This corresponding to a maximum moment of 39.19 t.m obtained from the spectrum analysis. On the other hand, the structural design has been performed for the maximum moment considering wind loading only which was calculated to be 19.1t.m.

Table 4.5 Maximum Moment Occurring at the Bottom of the GRP Section

| | | Damping | $M_{max}(t.m)$ |
|------------|-------------------|---------|----------------|
| Near Field | Time Analysis | 0.01 | - |
| | | 0.02 | - |
| | | 0.05 | - |
| | Spectrum Analysis | 0.01 | 130.90 |
| | | 0.02 | 88.95 |
| | | 0.05 | 69.85 |
| Far Field | Time Analysis | 0.01 | 62.45 |
| | | 0.02 | 51.53 |
| | | 0.05 | 32.05 |
| | Spectrum Analysis | 0.01 | 38.19 |
| | | 0.02 | 25.95 |
| | | 0.05 | 20.37 |

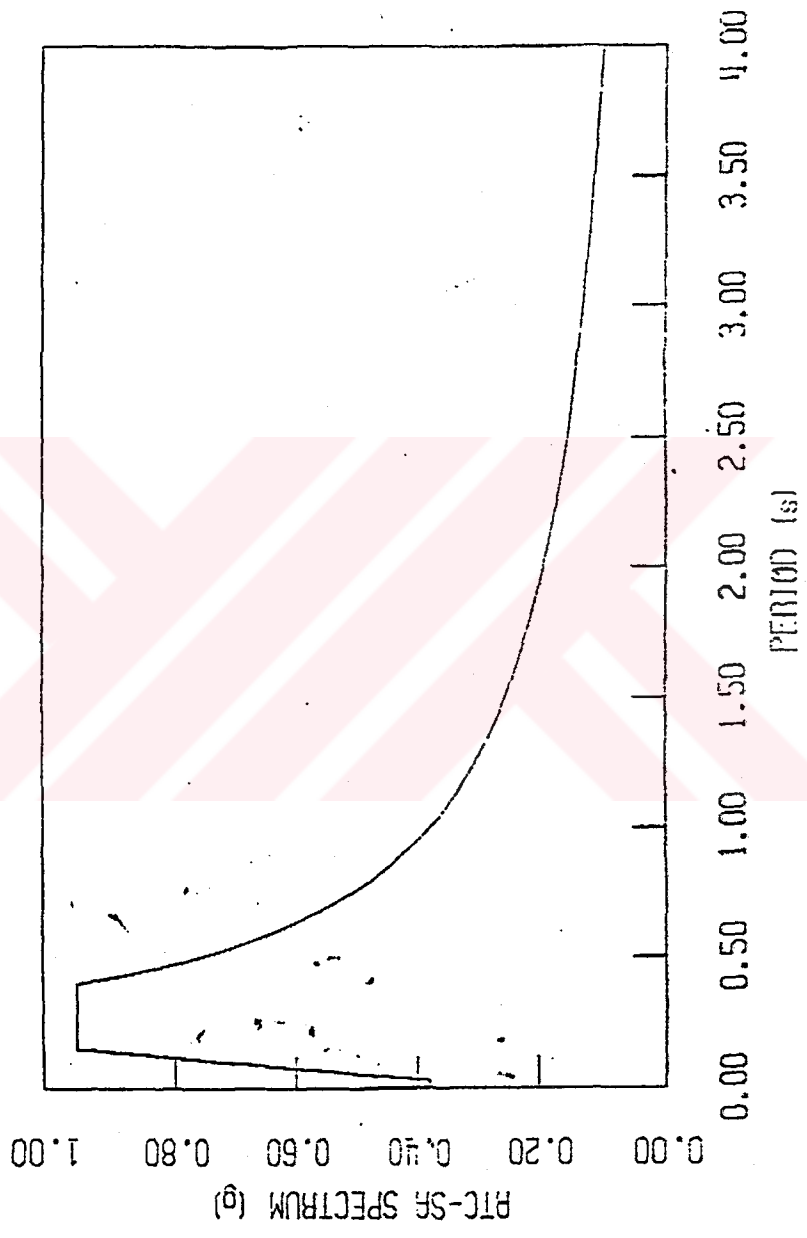


Figure 4.27 Near Field Design Response Spectrum, Damping 5%.

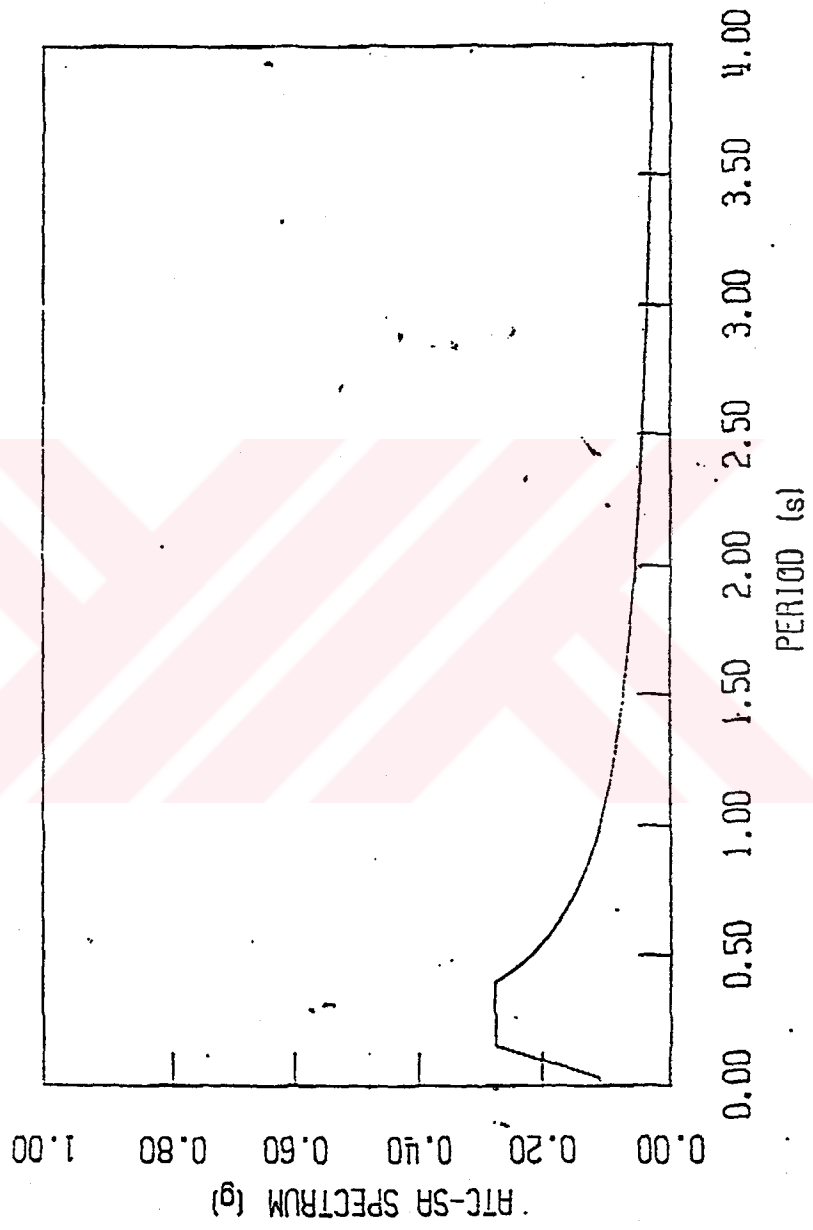


Figure 4.28 Far Field Design Response Spectrum, Damping 5%.

CHAPTER V

EQUIVALENT STATIC CALCULATIONS

5.1. General

It is a common practice in design codes to specify equivalent static lateral loading on various structures for estimating the earthquake response. Such an approach is considered useful for preliminary design because of its simplicity.

Although the exact nature of distribution of the equivalent lateral loads along the height of tower shaped structures is not yet known and can only be predicted by dynamic analysis, a careful static analysis may be enough for some structures.

There are different provisions for design of earthquake resistant structure using static loading and some of them is presented in this chapter. Aim of this presentation is to compare dynamic analysis with static equivalent calculations.

Table 5.1 Loads Along the Tower and Moments with respect to Elevations +0.00m, +14.10m, +30.00m, +60.90m and +82.10m

| Height | M. wrt +0.00 | M. wrt +14.10 | M. wrt +30.00 | M. wrt +60.90 | M. wrt +82.10 | Load |
|--------|--------------|---------------|---------------|---------------|---------------|----------|
| +0.00 | 0.00 | - | - | - | - | |
| +3.00 | 1,428.48 | - | - | - | - | 476.16 |
| +5.40 | 2,868.48 | - | - | - | - | 531.20 |
| +8.40 | 4,230.91 | - | - | - | - | 503.68 |
| +11.10 | 5,896.32 | - | - | - | - | 531.20 |
| +14.10 | 948.37 | 0.00 | - | - | - | 67.26 |
| +16.80 | 519.12 | 83.43 | - | - | - | 30.90 |
| +21.50 | 870.75 | 299.70 | - | - | - | 40.50 |
| +26.50 | 1,733.37 | 811.08 | - | - | - | 65.41 |
| +30.00 | 1,898.70 | 1,006.31 | 0.00 | - | - | 63.29 |
| +36.00 | 1,287.72 | 783.36 | 214.62 | - | - | 35.77 |
| +42.00 | 1,348.20 | 895.59 | 385.20 | - | - | 32.10 |
| +48.00 | 1,400.64 | 989.20 | 525.24 | - | - | 29.18 |
| +54.00 | 1,522.80 | 1,125.18 | 676.80 | - | - | 28.20 |
| +60.90 | 1,209.47 | 929.45 | 613.67 | 0.00 | - | 19.86 |
| +64.20 | 147.66 | 115.23 | 78.66 | 7.59 | - | 2.30 |
| +67.20 | 374.98 | 296.30 | 207.58 | 35.15 | - | 5.58 |
| +76.20 | 528.07 | 430.35 | 320.17 | 106.03 | - | 6.93 |
| +82.10 | 287.35 | 238.00 | 182.35 | 74.20 | 0.00 | 3.50 |
| +88.85 | 133.28 | 112.13 | 88.28 | 41.93 | 10.13 | 1.50 |
| +95.45 | 71.59 | 61.01 | 49.09 | 25.91 | 10.01 | 0.75 |
| Total | 28,706.26 | 8,176.32 | 3,341.66 | 290.81 | 20.14 | 2,475.27 |

For the static equivalent calculations of the tower, same masses as the dynamic analysis are used. Vertical loads and moments without seismic lateral load coefficient with respect to height along the tower are presented in Table 5.1

5.2 Design of Connections

It is advised that all parts of the building shall be interconnected and the connections shall be capable of transmitting the seismic force, F_p , induced by the parts being connected. As a minimum, any smaller portion of the building shall be tied to the remainder of the building with elements having at least a strength to resist $A_v/3$ times the weight of the smaller portion where A_v is the seismic coefficient representing the Effective Peak Velocity-Related Acceleration but not less than 5% of the portions weight[1].

Table 5.2 Coefficient A_v and Seismicity Index

| Map Area Number | Coefficient A_v | Seismicity Index |
|-----------------|-------------------|------------------|
| 7 | 0.40 | 4 |
| 6 | 0.30 | 4 |
| 5 | 0.20 | 4 |
| 4 | 0.15 | 3 |
| 3 | 0.10 | 2 |
| 2 | 0.05 | 2 |
| 1 | 0.05 | 1 |

As a minimum, a positive connection for resisting a horizontal force shall be provided for each appendage to its support which shall have a minimum strength acting along the span of the member equal to 5% of the dead and live load reaction.

Table 5.3 Minimum Load That Connections Should Resist

| Height of Connection | Weight of Smaller Portion (t) | (Av/3) x Weight (t) |
|----------------------|-------------------------------|---------------------|
| +30.00 | 197.32 | 13.15 |
| +60.90 | 40.42 | 2.69 |
| +82.10 | 5.75 | 0.38 |

The connections that holds the GRP antenna, should resist a 0.38t lateral load.

5.3 Equivalent Lateral Force Procedure

The general form of equivalent lateral force procedure is the Formula 5.1 for base shear, which gives the total seismic force F_b in terms of two factors, a seismic coefficient, C , and the total gravity load of the building, W .

$$F_b = C \cdot W \quad (5.1)$$

where

C = the seismic design coefficient

W = the total gravity load of the building

C can be calculated by different formulas according to different codes.

Here, the ATC 3-06 and Turkish codes are presented.

5.3.1 ATC 3-06 For Earthquake Resistant Structures

When the period of the building is computed, the seismic coefficient C_o shall be determined in accordance with the following formula:

$$C_o = \frac{1.2 A_v S}{R T^{\frac{2}{3}}} \quad (5.2)$$

where

A_v = the coefficient representing Effective Peak Velocity-Related Acceleration which can be taken as 0.20 for this case

S = the coefficient for the soil profile characteristics of the site which can be taken as 1.2 for this case

R = the response modification factor which is 4.50 for this case

$T =$ the fundamental period of the building, that may be determined based on the properties of the seismic resisting system in the direction of being analyzed and the use of the methods of mechanics assuming the base of the building to be fixed but shall not exceed $1.2T_a$. Alternatively the value of T , may be taken equal to the approximate fundamental period of the building, T_a , used to establish a minimum seismic base shear for the building.

The tower is nor a concrete neither a steel framing building so the equation at the below is used to calculate the fundamental period.

$$T_a = \frac{0.05h_n}{\sqrt{L}} \quad (5.4)$$

where $h_n =$ the height in feet above the base to the highest level of the building which is 313 feet for the tower

$L =$ the overall length in feet of the building at the base in the direction under consideration which is 46 feet for the tower

The fundamental period T , is calculated as 2.31 using above formulas, whereas the period computed at the ambient vibration tests and dynamic analysis were 1.81 and 1.799, respectively. The period that was calculated by static formulas, was used in static lateral load procedures.

The lateral seismic shear force F_x , induced at any level, shall be determined accordance with the following formula:

$$F_x = C_{vx} V \quad (5.4)$$

where

$$C_{vx} = \frac{w_x h_x^k}{\sum w_i h_i^k} \quad (5.5)$$

k is an exponent related to the building period as follows :

For buildings having a period of 0.5 seconds or less, $k = 1$

For buildings having a period of 2.5 seconds or more, $k = 2$

For the tower that have a period between 0.5 and 2.5 seconds, k is determined by linear interpolation between 1 and 2 and found to be 1.905.

w_i, w_x = the portion of W located at or assigned to level i or x .

h_i, h_x = the height above the base to level i or x

From above equations C can be determined as 0.037 and the lateral load distribution is presented in Table 5.4.

If the tower structure is taken as isolated from the building, then the total weight is about 520.27t and the lateral load is 2.37t. The lateral load

Table 5.4 Lateral Load Distribution Along the Tower According to ATC 3-06

| Height | Load | $W_i h_i$ | F_i |
|--------|--------|-----------|-------|
| +0.00 | | 0.00 | 0.00 |
| +3.00 | 30.90 | 92.70 | 0.14 |
| +5.40 | 30.90 | 166.86 | 0.26 |
| +8.40 | 30.90 | 259.56 | 0.40 |
| +11.10 | 30.90 | 342.99 | 0.52 |
| +14.10 | 30.90 | 435.69 | 0.67 |
| +16.80 | 30.90 | 519.12 | 0.79 |
| +21.50 | 40.50 | 870.75 | 1.33 |
| +26.50 | 65.41 | 1,733.37 | 2.65 |
| +30.00 | 63.29 | 1,898.70 | 2.90 |
| +36.00 | 35.77 | 1,287.72 | 1.97 |
| +42.00 | 32.10 | 1,348.20 | 2.06 |
| +48.00 | 29.18 | 1,400.64 | 2.14 |
| +54.00 | 28.20 | 1,522.80 | 2.33 |
| +60.90 | 19.86 | 1,209.47 | 1.85 |
| +64.20 | 2.30 | 147.66 | 0.23 |
| +67.20 | 5.58 | 374.98 | 0.57 |
| +76.20 | 6.93 | 528.07 | 0.81 |
| +82.10 | 3.50 | 287.35 | 0.44 |
| +88.85 | 1.50 | 133.28 | 0.20 |
| +95.45 | 0.75 | 71.59 | 0.11 |
| Total | 520.27 | 14,631.50 | 22.37 |

distribution along the stories is given in Table 5.4. The overturning moment calculated by the values at Table 5.4 at the base of the GRP section is 2.82tm.

5.3.2 Turkish Code For Earthquake Resistant Structures

When the period of the building is computed, the seismic coefficient C shall be determined in accordance with the following formula:

$$C = C_o \cdot K \cdot S \cdot I \quad (5.6)$$

where

- C_o = seismic zone coefficient which is 0.08 for II. Seismic Zone of Turkiye
- K = building type coefficient which is 2.0 for towers
- S = structural dynamic coefficient which is 1.0 maximum
- I = structural importance coefficient which is 1.50 for PTT buildings

From above equation the lateral load coefficient is calculated as 0.240 and distribution of the total lateral seismic load at any level may be calculated by the formula:

$$F_i = (F - F_t) \frac{W_i \cdot h_i}{\sum W_i \cdot h_i} \quad (5.7)$$

where

F = total lateral seismic load

W_i = vertical load of story i

h_i = height of the story i from the foundation level

F_t = lateral load applied on the top of the structure which will be

calculated by:

$$F_t = 0.004 \cdot F \left(\frac{H}{D} \right)^2 \quad (5.8)$$

where

H = height of the building which is 95.45m

D = width of the building at the foundation level which is about 14m

F_t can not be larger than 15% of F .

F_t is the term that may be used to include the second mode effects. In tower shaped structures, the second mode effect is not important so F_t should not be included.

If the tower structure is taken as isolated from the building, then the total weight is about 520.27t and the lateral load is 124.87t. The lateral load at the top story is not considered. The lateral load distribution along the stories is given in Table 5.5. The overturning moment calculated by the values at Table 5.4 at the base of the GRP section is 15.77 tm.

5.4 Cantilever Method

Inverted pendulum type structures like the tower being investigated are structures where the seismic resisting system acts essentially as an isolated cantilevers. Supporting columns or piers of inverted pendulum type structures shall be designed for the bending moment calculated at the base determined using the procedures of Equivalent Lateral Force Procedure for the base of the structure. One half of the calculated bending moment at the base is applied at the top and the moments along the column are varied from 1.5M at the base to 0.5M at the top. The addition of one half the moment calculated at the base is based on analysis of inverted pendulum covering a wide range of practical conditions.

Table 5.5 Lateral Load Distribution Along the Tower According to Turkish Code

| Height | Weight | $W_i h_i$ | F_i |
|--------|--------|-----------|--------|
| +3.00 | 30.90 | 92.70 | 0.79 |
| +5.40 | 30.90 | 166.86 | 1.42 |
| +8.40 | 30.90 | 259.56 | 2.21 |
| +11.10 | 30.90 | 342.99 | 2.92 |
| +14.10 | 30.90 | 435.69 | 3.70 |
| +16.80 | 30.90 | 519.12 | 4.41 |
| +21.50 | 40.50 | 870.75 | 7.40 |
| +26.50 | 65.41 | 1,733.37 | 14.73 |
| +30.00 | 63.29 | 1,898.70 | 16.14 |
| +36.00 | 35.77 | 1,287.72 | 10.95 |
| +42.00 | 32.10 | 1,348.20 | 11.46 |
| +48.00 | 29.18 | 1,400.64 | 11.91 |
| +54.00 | 28.20 | 1,522.80 | 12.94 |
| +60.90 | 19.86 | 1,209.47 | 10.28 |
| +64.20 | 2.30 | 147.66 | 1.26 |
| +67.20 | 5.58 | 374.98 | 3.19 |
| +76.20 | 6.93 | 528.07 | 4.49 |
| +82.10 | 3.50 | 287.35 | 2.44 |
| +88.85 | 1.50 | 133.28 | 1.13 |
| +95.45 | 0.75 | 71.59 | 0.61 |
| Total | 520.27 | 14,631.50 | 124.38 |

5.5. Strength Difference Method

ATC 3-06 states that large discontinuities in story strength can cause adverse response effects in a building. However, the usual practice is to determine what size, length, or strength of the resisting element is required (if more than the required strength is provided, so much the better), unfortunately, the extra strength in a story, if significantly different than that in adjacent stories, can produce responses which vary greatly from those calculated by using common procedures.

ATC 3-06 considers the following approach to this problem.

1. Compute the ratio of shear capacity to the design shear for each story. Denote this ratio for story n by r_n .
2. Compute r , the average r_n over all stories.
3. If for any story r_n is less than $(2/3)r$, modify R and C_d for the building, to $\sim R$ and $\sim C_d$ where

$$\sim C_d = 1 + \frac{C_d - 1}{2} \quad (5.9)$$

$$\sim R = \frac{\sim C_d}{C_d} R \quad (5.10)$$

4. Use $\sim R$ instead of R to recompute the lateral forces, and $\sim C_d$ instead of C_d in computing story drifts.

Table 5.6 Shear Capacity of Different Sections Along the Tower

| Height | A E (r_n) | r | $(^{2/3})r$ |
|-----------------|--------------------|-------------------|-------------------|
| +16.80 ~ +26.50 | 8.85×10^6 | 7.7×10^6 | 5.2×10^6 |
| +26.50 ~ +30.00 | 2.30×10^7 | | |
| +30.00 ~ +60.90 | 5.80×10^6 | | |
| +60.90 ~ +82.10 | 9.45×10^5 | | |
| +82.10 ~ | 3.8×10^4 | | |

Instead of the shear capacity ratio, AE is used and the results presented in Table 5.5.

$\sim C_b$ is computed as 2.5 and $\sim R$ is computed as 2.82. So, the coefficient C_o is comes to be 0.058, but not 0.037 and the Table 5.4 revised into Table 5.7. The overturning moment calculated by the values presented at Table 5.6 at the base of the GRP section is 4.63 tm.

5.6w. Japanese Practice

Society of Steel Construction of Japan, states that the lateral shear for any kind of appendages on buildings, q, shall be determined in accordance with formula

$$q = k W \quad (5.11)$$

where

k : seismic design coefficient for appendages which shall be 5 times the standard base shear coefficient, C_0

w : weight of appendage

The total weight of the GRP cylinder is about 2.50t and the lateral seismic load coefficient is about 0.240. Then, the seismic coefficient for the appendage and the overturning moment at the base of the GRP cylinder can be calculated easily. The seismic coefficient for appendage is 1.20 and the overturning moment is 121.0t.m by using the coefficient two times: first for the steel appendage on top of reinforced concrete and second for the GRP appendage on top of steel.

Table 5.7 Revised Lateral Loads Along the Tower with respect to Height

| Height | Load | $W_i h_i$ | F_i |
|--------|--------|-----------|-------|
| +0.00 | | 0.00 | 0.00 |
| +3.00 | 30.90 | 92.70 | 0.23 |
| +5.40 | 30.90 | 166.86 | 0.41 |
| +8.40 | 30.90 | 259.56 | 0.64 |
| +11.10 | 30.90 | 342.99 | 0.84 |
| +14.10 | 30.90 | 435.69 | 1.07 |
| +16.80 | 30.90 | 519.12 | 1.27 |
| +21.50 | 40.50 | 870.75 | 2.14 |
| +26.50 | 65.41 | 1,733.37 | 4.25 |
| +30.00 | 63.29 | 1,898.70 | 4.66 |
| +36.00 | 35.77 | 1,287.72 | 3.16 |
| +42.00 | 32.10 | 1,348.20 | 3.31 |
| +48.00 | 29.18 | 1,400.64 | 3.44 |
| +54.00 | 28.20 | 1,522.80 | 3.74 |
| +60.90 | 19.86 | 1,209.47 | 2.97 |
| +64.20 | 2.30 | 147.66 | 0.36 |
| +67.20 | 5.58 | 374.98 | 0.92 |
| +76.20 | 6.93 | 528.07 | 1.30 |
| +82.10 | 3.50 | 287.35 | 0.71 |
| +88.85 | 1.50 | 133.28 | 0.33 |
| +95.45 | 0.75 | 71.59 | 0.18 |
| Total | 520.27 | 14,631.50 | 22.37 |

CHAPTER VI

DISCUSSION OF THE RESULTS AND CONCLUSION

6.1. The Wind Loading Calculation by the Vendor

Wind load calculations were originally done for British Standard CP3, 1974 by ADC the vendor for GRP cylinders and presented as a report titled "Structural Analysis of Turkish Antenna GRP Cylinders"[19]. The wind speed is stated as 200 km/h, and this is utilized in the design.

Wind pressure according to BS-CP3 is calculated from

$$q = \frac{1}{2} \rho v^2 \quad (6.1)$$

for $\rho = 1225 \text{ kg/m}^3$ and $v = 200 \text{ km/hr} = 55.55 \text{ m/s}$ yielding $q = 1890 \text{ N/m}^2$.

The corresponding overturning moment at the bottom of the GRP section is calculated as 191 kN.m by assuming the bottom as a fixed base. The

design is performed for the maximum base moment using a longitudinal "instantaneous" modulus of elasticity of $E=1 \times 10^{10} \text{ N/m}^2$, a moment of inertia of $I=4.885 \times 10^{-3} \text{ m}^4$ and an outside diameter of $d=1.00 \text{ m}$. The stress at the bottom section of the GRP antenna was found as 0.199 t/cm^2 with a maximum fibre strain of 0.25% which is lower than the allowable fibre strain which is 0.375%. It was concluded that the GRP antenna portion of the tower is safe under wind loads.

Table 6.1 Comparison of Test and Computer Results

| | | 1st Mode | 2nd Mode | 3rd Mode | 4th Mode |
|------------------|----------------|----------|----------|----------|----------|
| Test Results | Frequency (Hz) | 0.55 | 1.28 | 2.25 | 3.24 |
| | Period (s) | 1.818 | 0.781 | 0.444 | 0.309 |
| Computer Results | Frequency (Hz) | 0.556 | 1.260 | 2.087 | 3.451 |
| | Period (s) | 1.799 | 0.794 | 0.479 | 0.290 |

6.2. Dynamic Analysis by Computer

The dynamic characters of the structure calculated by the tests are compared with the results of the computer model. The comparison of the results are presented in Table 6.1.

Comparison of test and computer results are perfect in first two modes

and pretty good in third and fourth modes. So the model may assumed that, it will show the load effects on the structure very well.

The tower was modelled like a cantilever bar that have the true stiffness and masses, and the shear walls were not modelled in detail. The model was not a detailed model in geometry but the masses and loads on the structure are tried to be perfect.

Comparing the two dynamic analysis methods, it was seen that time domain analysis gave higher load values that response spectrum analysis. This may arouse from an error in response spectrum analysis.

Comparison of the loads at the bottom section of the GRP antenna is presented in Table 6.2. The maximum overturning moment generated by the computer is 130.90tm which is nearly 6.7 times higher than the value held after the wind load calculations. At the assumed state of collapse, the overturning moment generated by the computer is 62.45tm which is 3.2 times higher than the wind load values. At the case of far field earthquake with 1% damping (that is considered as the state of collapse) the stress at the bottom of the GRP section is found as 0.639t/cm². This stress value is much more larger than the allowable stress.

6.3. Equivalent Static Calculations

Equivalent static calculations are investigated mainly using ATC 3_06 and Turkish Code. Also, using some regulations of Specifications of Society of Steel Construction of Japan[3], static calculations are presented.

Table 6.2 Comparison of Equivalent Static Calculations

| | Shear (t) | Moment (tm) |
|---|--------------|----------------|
| Design of Connections | 0.38 | - |
| Equivalent Lateral Force Procedure ATC 3-06 | 0.75 | 2.82 |
| Equivalent Lateral Force Procedure Turkish Regulations | 22.32 | 15.77 |
| Stiffness Difference Method | 1.22 | 4.63 |
| Cantilever Method | - | 171.40 |
| Society of Steel Construction of Japan | - | 121.0 |
| Dynamic Solution: | | |
| max, Near field earthquake, 1% damping | | 130.90 |
| state of collapse, Far field earthquake, 1% damping | | 62.45 |
| min, Far field earthquake, 5% damping | | 20.37 |

The results obtained from the computer model were 130.90tm maximum seismic moment at near field with 0.01 damping and 20.37tm minimum seismic moment at far field with 0.05 damping. Maximum stress at the bottom of the GRP antenna was found as 1.338t/cm^2 , and the stress was found as 0.638t/cm^2 at the

state of collapse which was assumed as the far field earthquake with damping value of 1%.

Equivalent static calculation results are presented in Table 6.2 and the results of computer model are presented in Table 6.3.

Table 6.3 Maximum Moment Occurring at the Bottom of the GRP Section

| | | Damping | M _{max} (t.m) |
|------------|-------------------|---------|------------------------|
| Near Field | Time Analysis | 0.01 | - |
| | | 0.02 | - |
| | | 0.05 | - |
| | Spectrum Analysis | 0.01 | 130.90 |
| | | 0.02 | 88.95 |
| | | 0.05 | 69.85 |
| Far Field | Time Analysis | 0.01 | 62.45 |
| | | 0.02 | 51.53 |
| | | 0.05 | 32.05 |
| | Spectrum Analysis | 0.01 | 38.19 |
| | | 0.02 | 25.95 |
| | | 0.05 | 20.37 |

The comparison between equivalent static calculations showed that every static calculation gave different results. But comparing the static solution results with

dynamic solution results it may be assumed that static calculations are useful for preliminary design only for special type of structures.

6.4. Conclusion

Model of the structure is prepared using correct masses and structural rigidities. Dynamic variables of the model is compared with the values of ambient vibration tests. Comparison of dynamic variables for the first two modes was perfect and also good for other modes. After this comparison, it may be assumed that the model demonstrates the real structure perfectly.

After comparing period and frequency values for different modes with computer model and ambient vibration test, confidence was gained about the mathematical model. The load values generated by computer model for near and far field earthquakes, different damping values and two different dynamic analysis methods are presented in Table 6.3.

Various static equivalent load calculations are used for the load values at the bottom of GRP antenna. For different methods of static calculations, completely different load values are obtained. Only, the calculations done by using the provisions presented by Society of Steel Construction of Japan, gave close

values to computer solution.

Calculations of the GRP cylinder presented by the vendor was examined. After considering all investigations about the tower, it may be said that the reason of the collapse was the underestimation of dynamic loads on the structure. The stress found at the base of the GRP antenna at far field earthquake with 1% damping was 0.639t/cm^2 which is 3.20 times higher than the maximum stress calculated by the vendor considering only wind loads. Calculations of the GRP cylinder made by the vendor was based on only static wind loads, and the dynamic characters of the structure were completely underestimated. This error in the calculation may arouse the collapse of the GRP antenna.

It may be said that by a simple model like the model that is used in this work, it is not very hard to get a real animation of a structure. Cantilever bar like computer models may be used in dynamic analysis of tower like structures also if the structure have great structural rigidity differences.

The load effects of special structures depend on their structural geometry with the characteristics of ground motion and the dynamic characteristics of the structure such as natural frequencies, mode shapes, and damping.

The response of special structures may be computed by complex and careful dynamic analysis requiring time wise superposition of responses in different modes of vibration. In response spectrum analysis, verification of the response spectrum is very important. Vibration characteristics and the dynamic properties of the tower shaped multi element structures are important design parameters controlling their earthquake safety. Any error in variables of response spectrum analysis is very important and may cause significant differences in results of the analysis.

The dual tower shaped structures are required to be designed for seismic forces particularly when they are located in moderate to severe seismic zones. Complete elastic response of tower shaped structures to earthquake motion can be computed only by dynamic analysis requiring time wise superposition of responses in different modes of vibration. However, it is a common practice in design codes to specify equivalent static lateral loading on various structures for estimating the earthquake response. Such an approach is considered useful for preliminary design because of its simplicity.

Although, it is a common practice to define static solutions equivalent to dynamic solutions, it is advised to use equivalent static loads for special structures only for preliminary design purposes. Exact response of such special buildings to

seismic effects may only be predicted by dynamic analysis. However, the exact nature of distribution of the equivalent lateral loads along the height of tower shaped structures is not yet known, a careful static analysis may be enough for some structures but not for tower shaped high rise structures which have structural rigidity differences between floors, and build with different types of materials.

Special type of structures, like towers, multi element structures, and the ones which have large stiffness differences within floors have to be designed for seismic forces particularly when they are located in moderate or severe seismic zones. The analysis of a structure and the provision of a design requirements are necessary to provide adequate earthquake resistance in structures.

REFERENCES

- [1].———, "ATC 3-06 : Tentative Provisions For The Development of Seismic Regulations for Buildings", Applied Technology Council, Berkeley, California, (June 1978)
- [2].———, "Seismic Design Guidelines For Essential Buildings", Department of the Army, (February 1986)
- [3].———, "Specifications for the Design, Fabrication & Erection of Steel Structures for Buildings", Society of Steel Construction of Japan, (June 1986)
- [4].———, "Symposium on Earthquake Engineering", University of Roorkee, (1974)
- [5].Bathe K.J., Wilson E.L., Peterson F.E., "SAPIV A Structural Analysis Program For Static and Dynamic Response of Linear Systems", (June 1973)

- [6].Craig, R.R.Jr., "Structural Dynamics", John Wiley & Sons, (1981)
- [7].Clough, R.W., Penzien J., "Dynamics of Structures", McGraw Hill International Editions, (1982)
- [8].Hansen, R.J., "Seismic Design for Nuclear Power Plants", The M.I.T. Press, (1979)
- [9].Juhasova, E., "Seismic Effects on Structures", Elsevier, (1991)
- [10].Unal, F., "Free Vibration Analysis of Suspension Bridges", A Master's Thesis in Civil Engineering, METU, (1989)
- [11].Wilson, E.L., "SOLID SAP A Static Analysis Program For Three Dimensional Solid Structures", CSI, (September 1971)
- [12].Wilson, E.L., Habibullah A., "SAP90 A Series of Computer Programs for the Static and Dynamic Finite Element Analysis of Structures", CSI, (1992)
- [13].Arya, A. S. and Thakkar, S. K., "Seismic Analysis of Hyperbolic Cooling Towers", Symposium on Earthquake Engineering, Roorkee, (November 1974)

- [14].Morrone, A., "Vibration of Stacks supported on Steel Structures", ASCE, Journal of Structural Division, (December 1969)
- [15].Korener, B. G., "Dynamics of Tower Structures", Bulletin of IASS, (March 1967)
- [16].Radhakrishnan R., "Frequency Response of Towershaped Structures", Symposium on Earthquake Engineering ,University of Roorkee, Roorkee, (November 1974)
- [17].Newton, D. A., "Vibration of Tower Frame Works", Publications of IABSE, (1971)
- [18].Yilmaz, Ç., Erdik, M., Akkaş, N., "Testing and Investigation of the TV Antennas with Special Emphasis on Kars Tower", Earthquake Engineering Research Center, METU, (September 1992)
- [19]. "Structural Analysis of Turkish Antenna GRP Cylinders" A Report prepared by Alan Dick & Company, September 1989.



APPENDICES

APPENDIX A

DYNAMIC ANALYSIS BY COMPUTER PROGRAM SAP90

A.1. Mode-Superposition Method

The equations of motion of a linear MDOF system is given by

$$m\ddot{u} + c\dot{u} + ku = p(t) \quad (\text{A.1})$$

In general, the coefficient matrices in Eq.(A.1), m , c , and k , may have non zero coupling terms (e.i. $k_{ij} = k_{ji} \neq 0$), so that to solve Eq.(A.1) in its present form would require simultaneous solution of N equations in N unknowns. Mode-superposition is a method by which such a set of coupled equations can be transformed into a set of uncoupled equations through use of the normal modes of the system.

Eq.(A.1) is the original set of coupled equations of motion for an N -DOF

system, where $u(t)$ may be physical or generalized coordinates. The response of the system to the excitation $p(t)$ and to the initial conditions

$$u(0) = u_0, \quad \dot{u}(0) = \dot{u}_0 \quad (\text{A.2})$$

is sought.

The first step in a mode-superposition solution is to obtain the natural frequencies and natural modes of the system. If all N nodes are to be considered, then the natural frequencies and modes satisfy

$$(k - \omega_r^2 m) \phi_r = 0 \quad (\text{A.3})$$

giving (ω_r^2, ϕ_r) , $r = 1, 2, \dots, N$. If the modes ϕ_r are assumed to have been normalized then modal mass, M_r and modal stiffness, K_r , calculated using

$$\begin{aligned} M_r &= \phi_r^T m \phi_r \\ K_r &= \omega_r^2 M_r \end{aligned} \quad (\text{A.4})$$

Assuming that if there are any repeated frequencies the associated modes have been orthogonalized so that the orthogonality equations

$$\phi_r^T m \phi_s = \phi_r^T k \phi_s = 0 \quad (\text{A.5})$$

are satisfied for all $r = s$. The modes are then collected to form the modal matrix Φ , that is,

$$\Phi = [\Phi_1 \ \Phi_2 \ \dots \ \Phi_N] \quad (\text{A.6})$$

The key step in the mode-superposition procedure is to introduce the coordinate transformation.

$$u(t) = \Phi \cdot \eta(t) = \sum_{r=1}^N \Phi_r \cdot \eta_r(t) \quad (\text{A.7})$$

The coordinates $\eta_r(t)$ will be referred to as principal coordinates. Eq.(A.7) is substituted into Eq.(A.1) and the resulting equation is multiplied by Φ^T to give the equation of motion in principal coordinates, namely

$$M\ddot{\eta} + C\dot{\eta} + K\eta = P(t) \quad (\text{A.8})$$

where

$$M = \Phi^T m \Phi = \text{modal mass matrix}$$

$$C = \Phi^T c \Phi = \text{modal damping matrix}$$

$$K = \Phi^T k \Phi = \text{modal stiffness matrix} \quad (\text{A.9})$$

$$P(t) = \Phi^T p(t) = \text{modal force matrix}$$

Due to the orthogonality conditions, of Eq.(A.5), M and K are diagonal matrices, so the equations of motion in modal coordinates, Eq.(A.8), are coupled only through nonzero off-diagonal coefficients in the modal damping matrix C.

The total response $\eta(t)$ can be obtained as a superposition of the response due to initial conditions alone and response due to the excitation alone.

$$\begin{aligned} u(0) &= \Phi \cdot \eta(0) \\ u(0) &= \Phi \cdot \eta(0) \end{aligned} \tag{A.10}$$

Multiplying these equations by Φ^T_m

$$\begin{aligned} \Phi^T_m u(0) &= M \eta(0) \\ \Phi^T_m u(0) &= M \eta(0) \end{aligned} \tag{A.11}$$

Since M is diagonal, Eq.(A.11) can be solved for the modal initial conditions giving

$$\begin{aligned} \eta_r(0) &= (1/M_r) \Phi_r^T u(0) \\ r &= 1, 2, \dots, N \end{aligned} \tag{A.12}$$

$$\eta_r(0) = (1/M_r) \Phi_r^T u(0)$$

A.2. Calculations of Frequencies and Mode Shapes

The dynamic analysis of a structural system using mode superposition requires the solution of the generalized eigenvalue problem, as the first step.

$$K \phi = \omega^2 M \phi \quad (\text{A.13})$$

where ω and ϕ are free vibration frequency and mode shape, respectively. The mass matrix is diagonal with partly zero diagonal elements. The program assumes that only the lowest p eigenvalues and corresponding eigenvectors are needed. The solution of Eq.(A.1) can therefore be written as

$$K \phi = M \phi \Omega^2 \quad (\text{A.14})$$

where Ω^2 is a diagonal matrix with the p smallest eigenvalues, i.e. $\Omega^2 = \text{diag}(\omega_1^2, \dots, \omega_p^2)$ and ϕ stores the corresponding M-orthonormalized eigenvectors $\phi_1, \phi_2, \dots, \phi_p$. Two different solution procedures are used in the program, a determinant search technique or a subspace iteration solution. The determinant search solution is carried out when the stiffness matrix can be contained in high-speed storage in one block. Therefore, for systems of large order and bandwidth, the subspace iteration method is used. Both solution techniques solve a transformation to the standard form.

A.3. The Determinant Search Solution

The determinant search technique is best suited for the analysis of large systems in which K and M have small bandwidths. Basically the solution algorithm combines triangular factorization and vector inverse iteration in an optimum manner to calculate the required eigenvalues and eigenvectors; these are obtained in sequence starting from the least dominant eigenpair w_1^2, Φ_1 . An efficient accelerated secant iteration procedure which operates on the characteristic polynomial.

$$p(w^2) = \det (K - w^2 M) \quad (\text{A.15})$$

is used to obtain a shift near the next unknown eigenvalue. The eigenvalue separation theorem is used in this iteration. Each determinant evaluation requires a triangular factorization of the matrix $K - w^2 M$. Once a shift near the unknown eigenvalue has been obtained, inverse iteration is used to calculate the eigenvector; the eigenvalue is obtained by adding the Rayleigh Quotient correction to the shift value.

A.4. The Subspace Iteration Solution

When the system is too large to be completely contained in high speed

storage, the subspace iteration solution is carried out. The iteration can be interpreted as a repeated application of the Ritz method, in which the computed eigenvectors from one step are used as a trial basis vectors for the next iteration until convergence to the required p eigenvalues and eigenvectors is obtained.

The solution is carried out by iterating simultaneously with q linearly independent vectors, where $q > p$. In the k 'th iteration the vectors span the q -dimensional subspace are calculated; i.e. when the vectors span the p -dimensional least dominant subspace, the required eigenvalues and eigenvectors are obtained.

Let v_0 store the starting vectors, then the k 'th iteration is described as follows:

Solve for vectors V_k which span ϵ_k

$$K V_k = M V_{k-1} \tag{A.16}$$

Calculate the properties of K and M onto ϵ_k

$$K_k = V_k^T K V_k \tag{A.17}$$

$$M_k = V_k^T M V_k \tag{A.18}$$

Solve for the eigensystem of K_k and M_k

$$K_k Q_k = M_k Q_k \Omega_k^2 \quad (\text{A.19})$$

and calculate the k 'th improved approximation to the eigenvectors

$$V_k = V_k Q_k \quad (\text{A.20})$$

Provided that the starting subspace is not orthogonal to any of the required eigenvectors, the iteration converges to the desired result. i.e. $\Omega_k^2 \rightarrow \Omega^2$ and $V_k \rightarrow \Phi$ as $k \rightarrow \infty$. The number of vectors q used in the iteration is taken greater than the desired number of eigenvectors in order to accelerate the convergence of the process. The number of iterations required to achieve satisfactory convergence depends, of course, on the quality of the starting vectors v_0 . Unless otherwise the program generates q starting vectors where $q = \min(2p, p+8)$, which has proven to be effective in general applications. At convergence a Sturm sequence check can be requested to verify that the lowest p eigenvalues have been found.

A.5. Dynamic Analysis

In dynamic response analysis the solution of the equations

$$M \ddot{u} + C \dot{u}_r + K u_r = R(t) \quad (\text{A.21})$$

is required, where $R(t)$ can be a vector of arbitrary time varying loads or of effective loads which result from ground motion. Specifically, in the case of ground motion, if it is assumed that the structure is uniformly subjected to the ground acceleration u_g , the equilibrium equations considered are

$$M \cdot u_r + C \cdot u_r + K \cdot u_r = -M \cdot u_g \quad (\text{A.22})$$

where u_r is the relative displacement of the structure with respect to the ground, i.e. $u_r = u - u_g$

The program can carry out a history analysis for solution of Eqs.(A.15) and (A.16), or a response spectrum analysis for solution of Eq.(A.16). The history analysis can be carried out using mode superposition or direct integration. The response spectrum analysis necessities, of course, first the solution of the required eigensystem.

A.6. Response History Analysis by Mode Superposition

In the mode superposition analysis, it is assumed that the structural response can be described adequately by the p lowest vibration modes, where $p \ll n$. Using the transformation $u = \Phi X$, where the columns in Φ are the p M -orthonormalized eigenvectors, Eq.(A.15) can be written as

$$X + \delta X + \Omega^2 X = \Phi^T R \quad (\text{A.23})$$

where

$$\delta = \text{diag}(2w_i \Gamma_i); \quad \Phi^2 = \text{diag}(w_i^2) \quad (\text{A.24})$$

In Eq.(A.18) it is that the damping matrix C satisfies the modal orthogonality condition

$$\Phi_i^T C \Phi_j = \delta_{ij} \quad (i = j) \quad (\text{A.25})$$

Eq.(A.17) therefore represents p uncoupled second order differential equations. These are solved in the program using the Wilson θ -Method, which is an unconditionally stable step-by-step integration scheme. The same time step is used in the integration of all equations to simplify the calculation of stress components at preselected times.

In the case of prescribed ground motion $u_g = \Phi X$ and in Eq.(A.17) the right hand side is given by $-\Phi^T.M.u_g$, where the ground acceleration is considered as the sum of the components in the x, y and z directions.

A.7. Response History Analysis by Direct Integration

The solution of the equations of motion, Eqs.(A.15) and (A.16), can be obtained by direct integration. In the program the Wilson θ -method is used, which is unconditionally stable. The algorithm employed is summarized in Table (A.1). This form of damping is easily taken account of in the analysis, because no storage and no multiplications for a damping matrix is required.

A.8. Response Spectrum Analysis

In this analysis the ground acceleration vector in Eq.(A.16) is written as

$$u_g = u_{gx} + u_{gy} + u_{gz} \quad (A.26)$$

where u_{gx} , u_{gy} and u_{gz} are the ground acceleration in the x, y and z directions, respectively. The equation for the response in the r'th mode is therefore

$$x_r + 2 \epsilon_r u_r x_r + u_r^2 x_r = r_{rx} + r_{ry} + r_{rz} \quad (A.27)$$

Table A.1 Step-by-Step Direct Integration Algorithm

Initial Calculations

1. Calculate the following constants

$$(\text{Assume } C = \alpha.M + \beta.K)$$

$$\Phi = 1.4, \quad \tau = \Theta \delta t$$

$$a_0 = (6 + 3\alpha\tau) / (\tau^2 + 3\beta\tau) \quad b_0 = \alpha - \beta a_0$$

$$a_1 = 6 / \tau^2 + 3b_0 / \tau \quad a_2 = 6 / \tau + 2b_0$$

$$a_3 = 2 + \tau b_0 / 2 \quad a_4 = 6 / [\Theta(38\tau + \tau^2)]$$

$$b_1 = \beta a_4$$

$$a_5 = 3b_1 / \tau + 6 / (\tau^2 + \Theta) \quad a_6 = 2b_1 - 6 / (\tau\Theta)$$

$$a_7 = (b_1 \tau / 2) + 1 - (3 / \Theta) \quad a_8 = \delta t / 2$$

$$a_9 = \delta t^2 / 3 \quad a_{10} = (1/2) a_9$$

2. Form effective stiffness matrix $K^* = K + a_0 M$
3. Triangularize K_*

For Each Time Increment

1. Form effective load vector R_t^*

$$R_t^* = R_t - \Theta(R_{t+\delta t} - R_t) + M(a_1 u_t + a_2 \dot{u}_t + a_3 \ddot{u}_t)$$

2. Solve for effective displacement vector u_t^*

$$K^* u_t^* = R_t^*$$

3. Calculate new acceleration, velocity and displacement vectors,

$$u_{t+\delta t} = a_4 u_t + a_5 \dot{u}_t + a_6 \ddot{u}_t + a_7 u_t$$

$$u_{t+\delta t} = u_t - a_8 (u_{t+\delta t} - u_t)$$

$$u_{t+\delta t} = u_t + \delta t u_t + a_9 u_t + a_{10} u_{t+\delta t}$$

4. Calculate element stresses if desired where x_r is the r 'th element in X and

$$r_{rx} = -\phi_r^T \cdot M \cdot u_{gx}; r_{ry} = -\phi_r^T \cdot M \cdot u_{gy}; r_{rz} = -\phi_r^T \cdot M \cdot u_{gz}$$

Using the definition of the spectral displacement, the maximum absolute modal displacements of the structure subjected to an acceleration into the x direction are

$$r_{rx}^{(max)} = \phi_r | \phi_r^T \cdot M \cdot I_x | S_x (w_r) \quad (A.28)$$

where $S_x (w_r)$ is the spectral displacement into the x direction corresponding to the frequency w_r and I_x is a null vector except that those elements are equal to one which correspond to the x -translational degrees of freedom. Similarly, for the responses due to a ground acceleration into y and z -directions

$$u_{ry}^{(max)} = \phi_r | \phi_r^T \cdot M \cdot I_y | S_y (w_r) \quad (A.29)$$

$$u_{rz}^{(max)} = \phi_r | \phi_r^T \cdot M \cdot I_z | S_z (w_r) \quad (A.30)$$

and the total maximum response in the r 'th mode is assumed to be

$$u_r^{(\max)} = u_{rx}^{(\max)} + u_{ry}^{(\max)} + u_{rz}^{(\max)} \quad (\text{A.31})$$

Program SAP90 calculates the maximum responses in each of the p lowest modes, where the spectra (displacements or acceleration) into the x , y and z -directions are assumed to be proportional to each other. The total response for displacements and stress resultants is calculated as the square root of the sum of the squares of the modal maximum responses.

APPENDIX B

COMPUTER INPUT FOR SAP90

The computer model input prepared by an ASCII editor is given at below:

PTT KARS TV ANTENNA DYNAMIC ANALYSIS

SYSTEM

N=1517 V=8

JOINTS

1 X=+6.727 Y=+1.531 Z=0.000

2 X=+5.401 Y=+4.291

3 X=+3.010 Y=+6.206

4 X=+0.022 Y=+6.897

5 X=-2.971 Y=+6.224

6 X=-5.382 Y=+4.314

7 X=-6.725 Y=+1.541

- 8 X=-6.725 Y=-1.541
- 9 X=-5.382 Y=-4.319
- 10 X=-2.971 Y=-6.224
- 11 X=+0.022 Y=-6.897
- 12 X=+3.010 Y=-6.206
- 13 X=+5.401 Y=-4.291
- 14 X=+6.727 Y=-1.531
- 15 X=-1.600 Y=+0.000
- 101 X=+6.727 Y=+1.531 Z=3.000
- 102 X=+5.401 Y=+4.291
- 103 X=+3.010 Y=+6.206
- 104 X=+0.022 Y=+6.897
- 105 X=-2.971 Y=+6.224
- 106 X=-5.382 Y=+4.314
- 107 X=-6.725 Y=+1.541
- 108 X=-6.725 Y=-1.541
- 109 X=-5.382 Y=-4.319
- 110 X=-2.971 Y=-6.224
- 111 X=+0.022 Y=-6.897
- 112 X=+3.010 Y=-6.206
- 113 X=+5.401 Y=-4.291

114 X=+6.727 Y=-1.531
115 X=-1.600 Y=+0.000
201 X=+6.727 Y=+1.531 Z=5.400
202 X=+5.401 Y=+4.291
203 X=+3.010 Y=+6.206
204 X=+0.022 Y=+6.897
205 X=-2.971 Y=+6.224
206 X=-5.382 Y=+4.314
207 X=-6.725 Y=+1.541
208 X=-6.725 Y=-1.541
209 X=-5.382 Y=-4.319
210 X=-2.971 Y=-6.224
211 X=+0.022 Y=-6.897
212 X=+3.010 Y=-6.206
213 X=+5.401 Y=-4.291
214 X=+6.727 Y=-1.531
215 X=-1.600 Y=+0.000
301 X=+6.727 Y=+1.531 Z=8.600
302 X=+5.401 Y=+4.291
303 X=+3.010 Y=+6.206
304 X=+0.022 Y=+6.897

T.C. YÜKSEKÖĞRETİM KURULU
DOKÜMANTASYON MERKEZİ

305 X=-2.971 Y=+6.224
306 X=-5.382 Y=+4.314
307 X=-6.725 Y=+1.541
308 X=-6.725 Y=-1.541
309 X=-5.382 Y=-4.319
310 X=-2.971 Y=-6.224
311 X=+0.022 Y=-6.897
312 X=+3.010 Y=-6.206
313 X=+5.401 Y=-4.291
314 X=+6.727 Y=-1.531
315 X=-1.600 Y=+0.000
401 X=+6.727 Y=+1.531 Z=11.300
402 X=+5.401 Y=+4.291
403 X=+3.010 Y=+6.206
404 X=+0.022 Y=+6.897
405 X=-2.971 Y=+6.224
406 X=-5.382 Y=+4.314
407 X=-6.725 Y=+1.541
408 X=-6.725 Y=-1.541
409 X=-5.382 Y=-4.319
410 X=-2.971 Y=-6.224

411 X=+0.022 Y=-6.897
412 X=+3.010 Y=-6.206
413 X=+5.401 Y=-4.291
414 X=+6.727 Y=-1.531
415 X=-1.600 Y=+0.000
501 X=+6.727 Y=+1.531 Z=14.100
502 X=+5.401 Y=+4.291
503 X=+3.010 Y=+6.206
504 X=+0.022 Y=+6.897
505 X=-2.971 Y=+6.224
506 X=-5.382 Y=+4.314
507 X=-6.725 Y=+1.541
508 X=-6.725 Y=-1.541
509 X=-5.382 Y=-4.319
510 X=-2.971 Y=-6.224
511 X=+0.022 Y=-6.897
512 X=+3.010 Y=-6.206
513 X=+5.401 Y=-4.291
514 X=+6.727 Y=-1.531
515 X=-1.600 Y=+0.000
527 Z=+26.000 G=515,527,1

| | | |
|-----|------------|-------------|
| 531 | Z= +30.000 | G=527,531,1 |
| 562 | Z= +60.900 | G=531,562,1 |
| 583 | Z= +82.100 | G=562,583,1 |
| 598 | Z= +97.000 | G=583,598,1 |

RESTRAINTS

1 15 1 R=1,1,1,1,1,1
101 115 1 R=0,0,0,0,0,0
201 215 1 R=0,0,0,0,0,0
301 315 1 R=0,0,0,0,0,0
401 415 1 R=0,0,0,0,0,0
501 598 1 R=0,0,0,0,0,0

CONSTRAINTS

101 114 1 C=115,115,0,0,0,0
201 214 1 C=215,215,0,0,0,0
301 314 1 C=315,315,0,0,0,0
401 414 1 C=415,415,0,0,0,0
501 514 1 C=515,515,0,0,0,0

FRAME

NM=12

1 A=0.15 I=0.00100,0.00300 M=0.110 E=2.7E6 : Reinf.Concrete
2 A=3.336 I=7.55900,7.55900 J=0.0001 M=0.850 :
3 A=14.13 I=19.8700,19.8700 J=0.0001 M=3.432
4 A=2.755 I=1.37900,1.37900 J=0.0001 M=0.702
5 A=2.600 I=1.32600,1.32600 J=0.0001 M=0.662
6 A=2.444 I=1.27300,1.27300 J=0.0001 M=0.623
7 A=2.289 I=1.21900,1.21900 J=0.0001 M=0.583
8 A=2.133 I=1.11600,1.11600 J=0.0001 M=0.544
9 A=1.978 I=1.11300,1.11300 J=0.0001 M=0.504
10 A=0.067 I=0.18700,0.18700 J=0.00001 M=0.105 E=2.1E7 : Steel
11 A=0.038 I=0.00488,0.00488 J=0.00001 M=0.020 E=0.9E6 : GRP
12 A=0.04 I=0.00013,0.00013 E=2.7E6 : 20x20 Column

C MAIN TOWER

1 15 115 M=2 LP=2,0
2 115 215
3 215 315
4 315 415
5 415 515
6 515 516 G=11,1,1,1
18 527 528 M=3 G=3,1,1,1

| | | | | |
|----|-----|-----|------|------------|
| 22 | 531 | 532 | M=4 | G=4,1,1,1 |
| 27 | 536 | 537 | M=5 | G=4,1,1,1 |
| 32 | 541 | 542 | M=6 | G=4,1,1,1 |
| 37 | 546 | 547 | M=7 | G=4,1,1,1 |
| 42 | 551 | 552 | M=8 | G=4,1,1,1 |
| 47 | 556 | 557 | M=9 | G=5,1,1,1 |
| 53 | 562 | 563 | M=10 | G=20,1,1,1 |
| 74 | 583 | 584 | M=11 | G=14,1,1,1 |

C 20x20 COLUMNS

| | | | | |
|-----|----|-----|-------------|-----------------|
| 101 | 1 | 101 | M=12 LP=2,0 | G=4,100,100,100 |
| 102 | 2 | 102 | | G=4,100,100,100 |
| 103 | 3 | 103 | | G=4,100,100,100 |
| 104 | 4 | 104 | | G=4,100,100,100 |
| 105 | 5 | 105 | | G=4,100,100,100 |
| 106 | 6 | 106 | | G=4,100,100,100 |
| 107 | 7 | 107 | | G=4,100,100,100 |
| 108 | 8 | 108 | | G=4,100,100,100 |
| 109 | 9 | 109 | | G=4,100,100,100 |
| 110 | 10 | 110 | | G=4,100,100,100 |
| 111 | 11 | 111 | | G=4,100,100,100 |
| 112 | 12 | 112 | | G=4,100,100,100 |

113 13 113 G=4,100,100,100

114 14 114 G=4,100,100,100

C 20x20 BEAMS

121 101 102 LP=1,0 G=3,100,100,100

122 102 103 G=3,100,100,100

123 103 104 G=3,100,100,100

124 104 105 G=3,100,100,100

125 105 106 G=3,100,100,100

126 106 107 G=3,100,100,100

127 107 108 G=3,100,100,100

128 108 109 G=3,100,100,100

129 109 110 G=3,100,100,100

130 110 111 G=3,100,100,100

131 111 112 G=3,100,100,100

132 112 113 G=3,100,100,100

133 113 114 G=3,100,100,100

134 114 101 G=3,100,100,100

C FLOOR BEAMS

1101 101 115 M=1 LP=1,0 RE=0,2.125

1111 114 115 RE=0,2.125

1102 102 115 RE=0,2.125

| | | | | |
|------|-----|-----|-----|------------|
| 1112 | 113 | 115 | | RE=0,2.125 |
| 1103 | 103 | 115 | | RE=0,2.125 |
| 1113 | 112 | 115 | | RE=0,2.125 |
| 1104 | 104 | 115 | | RE=0,2.125 |
| 1114 | 111 | 115 | | RE=0,2.125 |
| 1105 | 105 | 115 | | RE=0,2.125 |
| 1115 | 110 | 115 | | RE=0,2.125 |
| 1106 | 106 | 115 | | RE=0,2.125 |
| 1116 | 109 | 115 | | RE=0,2.125 |
| 1107 | 107 | 115 | | RE=0,2.125 |
| 1117 | 108 | 115 | | RE=0,2.125 |
| 1201 | 201 | 215 | M=1 | RE=0,2.125 |
| 1211 | 214 | 215 | | RE=0,2.125 |
| 1202 | 202 | 215 | | RE=0,2.125 |
| 1212 | 213 | 215 | | RE=0,2.125 |
| 1203 | 203 | 215 | | RE=0,2.125 |
| 1213 | 212 | 215 | | RE=0,2.125 |
| 1204 | 204 | 215 | | RE=0,2.125 |
| 1214 | 211 | 215 | | RE=0,2.125 |
| 1205 | 205 | 215 | | RE=0,2.125 |
| 1215 | 210 | 215 | | RE=0,2.125 |

| | | |
|--------------|-----|------------|
| 1206 206 215 | | RE=0,2.125 |
| 1216 209 215 | | RE=0,2.125 |
| 1207 207 215 | | RE=0,2.125 |
| 1217 208 215 | | RE=0,2.125 |
| 1301 301 315 | M=1 | RE=0,2.125 |
| 1311 314 315 | | RE=0,2.125 |
| 1302 302 315 | | RE=0,2.125 |
| 1312 313 315 | | RE=0,2.125 |
| 1303 303 315 | | RE=0,2.125 |
| 1313 312 315 | | RE=0,2.125 |
| 1304 304 315 | | RE=0,2.125 |
| 1314 311 315 | | RE=0,2.125 |
| 1305 305 315 | | RE=0,2.125 |
| 1315 310 315 | | RE=0,2.125 |
| 1306 306 315 | | RE=0,2.125 |
| 1316 309 315 | | RE=0,2.125 |
| 1307 307 315 | | RE=0,2.125 |
| 1317 308 315 | | RE=0,2.125 |
| 1401 401 415 | M=1 | RE=0,2.125 |
| 1411 414 415 | | RE=0,2.125 |
| 1402 402 415 | | RE=0,2.125 |

| | | |
|--------------|-----|------------|
| 1412 413 415 | | RE=0,2.125 |
| 1403 403 415 | | RE=0,2.125 |
| 1413 412 415 | | RE=0,2.125 |
| 1404 404 415 | | RE=0,2.125 |
| 1414 411 415 | | RE=0,2.125 |
| 1405 405 415 | | RE=0,2.125 |
| 1415 410 415 | | RE=0,2.125 |
| 1406 406 415 | | RE=0,2.125 |
| 1416 409 415 | | RE=0,2.125 |
| 1407 407 415 | | RE=0,2.125 |
| 1417 408 415 | | RE=0,2.125 |
| 1501 501 515 | M=1 | RE=0,2.125 |
| 1511 514 515 | | RE=0,2.125 |
| 1502 502 515 | | RE=0,2.125 |
| 1512 513 515 | | RE=0,2.125 |
| 1503 503 515 | | RE=0,2.125 |
| 1513 512 515 | | RE=0,2.125 |
| 1504 504 515 | | RE=0,2.125 |
| 1514 511 515 | | RE=0,2.125 |
| 1505 505 515 | | RE=0,2.125 |
| 1515 510 515 | | RE=0,2.125 |

1506 506 515 RE=0,2.125

1516 509 515 RE=0,2.125

1507 507 515 RE=0,2.125

1517 508 515 RE=0,2.125

MASSES

583 M=1.000,1.000

562 M=1.000,1.000

SHELL

NM=1

1 U=0.20 M=0.051 E=2.65E6

1 JQ= 1, 2,101,102 ETYPE=0 M=1 TH=0.20 LP=0 G=13,1

14 JQ= 14, 1,114,101

101 JQ=101,102,201,202 G=13,1

114 JQ=114,101,214,201

201 JQ=201,202,301,302 G=13,1

214 JQ=214,201,314,301

301 JQ=301,302,401,402 G=13,1

314 JQ=314,301,414,401

401 JQ=401,402,501,502 G=13,1

414 JQ=414,401,514,501